Available online at www.sciencedirect.com
SCIENCE DIRECT®
Developmental Biology 267 (2004) 342–360
DEVELOPMENTAL BIOLOGY
www.elsevier.com/locate/ydbio

Fundamental properties of the spiralian developmental program are displayed by the basal nemertean *Carinoma tremaphoros* (Palaeonemertea, Nemertea)

Svetlana A. Maslakova,[a,b,*] Mark Q. Martindale,[c] and Jon L. Norenburg[b]

[a] *Department of Biology, The George Washington University, 2023 G Street NW, Washington, DC 20052, USA*
[b] *National Museum of Natural History, Smithsonian Institution, MRC 163, PO BOX 37012, Washington, DC 20013-7012, USA*
[c] *Kewalo Marine Laboratory, Pacific Biomedical Research Center, University of Hawaii, Honolulu, HI 96813, USA*

Received for publication 16 December 2002, revised 13 October 2003, accepted 15 October 2003

Abstract

The first description of the cleavage program of the palaeonemertean *Carinoma tremaphoros* (a member of a basal clade of the Nemertea) is illustrated by confocal microscopy and microinjection and compared to development of more derived nemerteans and other eutrochozoans (Annelida, Mollusca, Sipunculida and Echiurida). Lineage tracers were injected into individual blastomeres of *C. tremaphoros* at the 2-, 4-, 8- and 16-cell stage. Subsequent development was followed to the formation of simple (so-called planuliform) planktonic larvae to establish the ultimate fates of the blastomeres. Results of labeling experiments demonstrate that the development of *C. tremaphoros* bears closer similarity to other Eutrochozoa than development of a previously studied hoplonemertean (*Nemertopsis bivittata*) and a heteronemertean (*Cerebratulus lacteus*) in that the first cleavage plane bears an invariant relationship to the plane of bilateral symmetry of the larval body. Additionally, our cell-labeling experiments support the earlier suggestion that the transitory pre-oral belt of cells in the larvae of *C. tremaphoros* corresponds to the prototroch of other Eutrochozoa. A unique feature of development of *C. tremaphoros* includes the oblique orientation of the trochal lineages with respect to the anterior–posterior axis of the larva. The significance and application of cleavage characters such as presence of molluscan vs. annelid cross for phylogenetic analyses is reviewed. We argue that molluscan or annelid cross, neither of which are present in nemerteans, are merely two out of much greater variety of patterns created by the differences in the relative size and timing of formation of micromere quartets and none can be considered, by itself, as evidence of close phylogenetic relationship between phyla.

Keywords: Nemertean; Spiral cleavage; Cell lineage; Prototroch; Molluscan cross; Annelid cross

Introduction

Nemerteans belong to a large clade of protostome coelomates, the Eutrochozoa, along with the Annelida, Echiurida, Sipunculida and Mollusca. Despite the recent surge of phylogenetic analyses of the Metazoa, the evolutionary relationships within the major groups, such as Eutrochozoa remain controversial (Jenner and Schram, 1999; Nielsen, 2001; Peterson and Eernisse, 2001). Recent experiments on the early development of various eutrochozoans have revealed certain differences in the contributions of the embryonic cells to the larval and adult structures that might reflect the evolutionary relationships of these organisms. The suggested basal position of nemerteans within the Eutrochozoa (Peterson and Eernisse, 2001) and diversity of developmental modes within this group makes nemerteans an excellent group for comparative evolutionary developmental studies. However, due to the scarcity of information on their early embryonic and larval development, nemerteans have received little attention in the discussion of the ancestral mode of the development and evolution of protostome coelomates. The development of palaeonemerteans (Palaeonemertea; Nemertea) is of particular interest because this group appears to be the most basal among nemerteans (Norenburg and Stricker, 2002; Thollesson and Norenburg, 2003) and is thus likely to provide important insights into the ancestral mode of nemertean, and perhaps, Eutrochozoan development. However, compared to the better-studied heteronemerteans (e.g., *Cerebratulus*) and to a lesser extent hoplonemerteans (e.g., *Nemertopsis*), early

* Corresponding author. Fax: +1-202-357-3043.
E-mail address: maslak@gwu.edu (S.A. Maslakova).

0012-1606/$ - see front matter © 2003 Elsevier Inc. All rights reserved.
doi:10.1016/j.ydbio.2003.10.022

development of palaeonemerteans remains largely undescribed (Friedrich, 1979; Henry and Martindale, 1997; Iwata, 1960; Norenburg and Stricker, 2002 and references therein).

Nemerteans possess equal holoblastic spiral cleavage. One of the unusual characteristics of nemertean cleavage is inversion of the sizes of micro- and macromeres at the eight-cell stage. Similar to sipunculids, but unlike most other eutrochozoans, the first-quartet micromeres at the eight-cell stage are of equal size or larger than the corresponding vegetal macromeres (Friedrich, 1979; Rice, 1985). This results in a visible shift of the quadrant domains in the larval ectoderm, compared to other Eutrochozoa, as most of nemertean larval ectoderm is derived from the first-quartet micromeres (Henry and Martindale, 1998). Late onset of bilateral symmetry is another distinguishing feature of nemertean cleavage. In typical equal spiral cleavage, bilateral symmetry is established after formation of the 4d blastomere, which divides bilaterally to produce two mesoteloblasts. In nemerteans, radial symmetry persists until the beginning of the gastrulation and division of fourth-quartet micromeres and macromeres cannot be observed, as they gastrulate first (Delsman, 1915). Recent advances in experimental embryology stimulated a series of cell lineage studies on the members of Eutrochozoa (Boyer et al., 1998; Dictus and Damen, 1997; Henry and Martindale, 1998; Render, 1997). These studies proved that despite the great conservatism of the spiral cleavage program considerable differences exist between the exact contributions of identified blastomeres to larval/adult structures among members of the Eutrochozoa (Boyer and Henry, 1998; Henry and Martindale, 1999). Experiments on the development of the hoplonemertean *Nemertopsis bivittata* and the heteronemertean *Cerebratulus lacteus* revealed that unlike the case in the annelids and mollusks, in which the first cleavage plane bears a strict 45 ° angular relationship to the future dorso-ventral axis, the first cleavage plane in the nemertean development can bear one of two different relationships relative to the larval plane of bilateral symmetry (Henry and Martindale, 1994, 1998). The question remains how conclusive these results are in terms of the ancestral condition within the Nemertea and Eutrochozoa.

The stereotyped and highly conservative cleavage program in spiralian embryos allows for the identification of homologous cells between different animal phyla. A sophisticated system of nomenclature had been developed for spiralian embryos to trace fates of individual blastomeres (Wilson, 1892; modified by Child, 1900). Significant weight had been given to some of the early cleavage characters, for example, a stereotyped cross-like apical pattern, formed by the progeny of the 1st and 2nd quartet micromeres—the so-called molluscan and annelid cross (McBride, 1914; Pilger, 1997). For example, the shared presence of a molluscan cross in mollusks and sipunculids and an annelid cross in annelids and echiurids is sometimes used to imply close evolutionary relationships between these groups (Pilger, 1997; Rice, 1985; Scheltema, 1993). However, a detailed analysis of the cleavage program of a large sample of spiralian embryos reveals that the presence of a molluscan or annelid cross is merely two out of a much greater variety of patterns created by the differences in the relative size and timing of formation of micromere quartets. Here, we use confocal microscopy to describe in detail for the first time the early cleavage program of the palaeonemertean *Carinoma tremaphoros* up through the cleavages giving rise to the ‘‘cross’’. We compare the development of this basal nemertean to development of mollusks, annelids, sipunculids and other nemerteans, and discuss the significance of cleavage characters in the evolution of development of the Eutrochozoa.

Material and methods

Collecting adults and obtaining gametes

C. tremaphoros is a common littoral species near the Smithsonian Marine Station at Fort Pierce, FL (SMSFP). Reproductive specimens of *C. tremaphoros* were collected February through May, 2001 and in March, 2002 in the top 10–15 cm of sand at the low tide mark—approximately at the upper edge of the *Halodule wrightii* (shoal grass) zone. The collecting site—a sand flat on the eastern bank of the Indian River Lagoon just south of the SMSFP becomes regularly exposed during the low tides. Adults can survive for several weeks in the laboratory when kept at the room temperature in a large bowl with sand, covered by about 2–3 cm of seawater. Animals, however, quickly die if left in seawater without sediment. Ripe males and females were dissected to obtain gametes. Each female produces up to a few hundreds of eggs. Eggs were fertilized by adding a drop of sperm diluted in seawater (1:1000) to 10–15 ml of filtered seawater containing eggs.

Early cleavage and confocal microscopy

The timing of early development was recorded for 15–20 embryos from five batches of eggs. Early cleavage was studied in vivo with a Zeiss stereomicroscope. Because of the small size of the embryos, cells become hard to identify after about 32-cell stage with these optics. For confocal microscopy, some embryos were fixed for 30–40 min in 4% paraformaldehyde in phosphate buffer saline (PBS) at room temperature, washed and stored in PBS at 4 °C. Alternatively, embryos were fixed in Zenker’s solution (Carson, 1990) for 1 h, rinsed in tap water and stored in 70% ethanol. All embryos were subsequently dehydrated in an isopropyl alcohol series and mounted in 1:2 benzyl alcohol to benzyl benzoate. Slides for mounting were pretreated with 0.1% poly-L-lysine solution to prevent embryos from rolling during the confocal microscopy session. Mounts were viewed on a Zeiss compound microscope with LSM 510

Zeiss confocal system with Argon laser (488 nm emission). Yolk autofluorescence provided sufficient signal without additional staining.

Cell lineage analysis via microinjected fluorescent tracers

Embryonic chorions were removed with sharp forceps to facilitate the injections. Embryos were then placed in small Petri dishes that had been coated with gelatin to prevent the denuded cells from sticking to the plastic surface (Henry and Martindale, 1998). To immobilize them for injection, embryos were rolled into the shallow groves that had been etched into the bottoms of gelatin-coated dishes using a small piece of broken glass. Fluorescent lineage tracers, either lipophilic DiI (Molecular Probes, Inc.) dissolved in vegetable oil (Henry and Martindale, 1998) or lysinated tetramethylrhodamine (Fluororuby) (Molecular Probes, Inc.) were directly injected in the individual blastomeres at the two-, four- or eight-cell stages. Embryos that survived microinjection continued

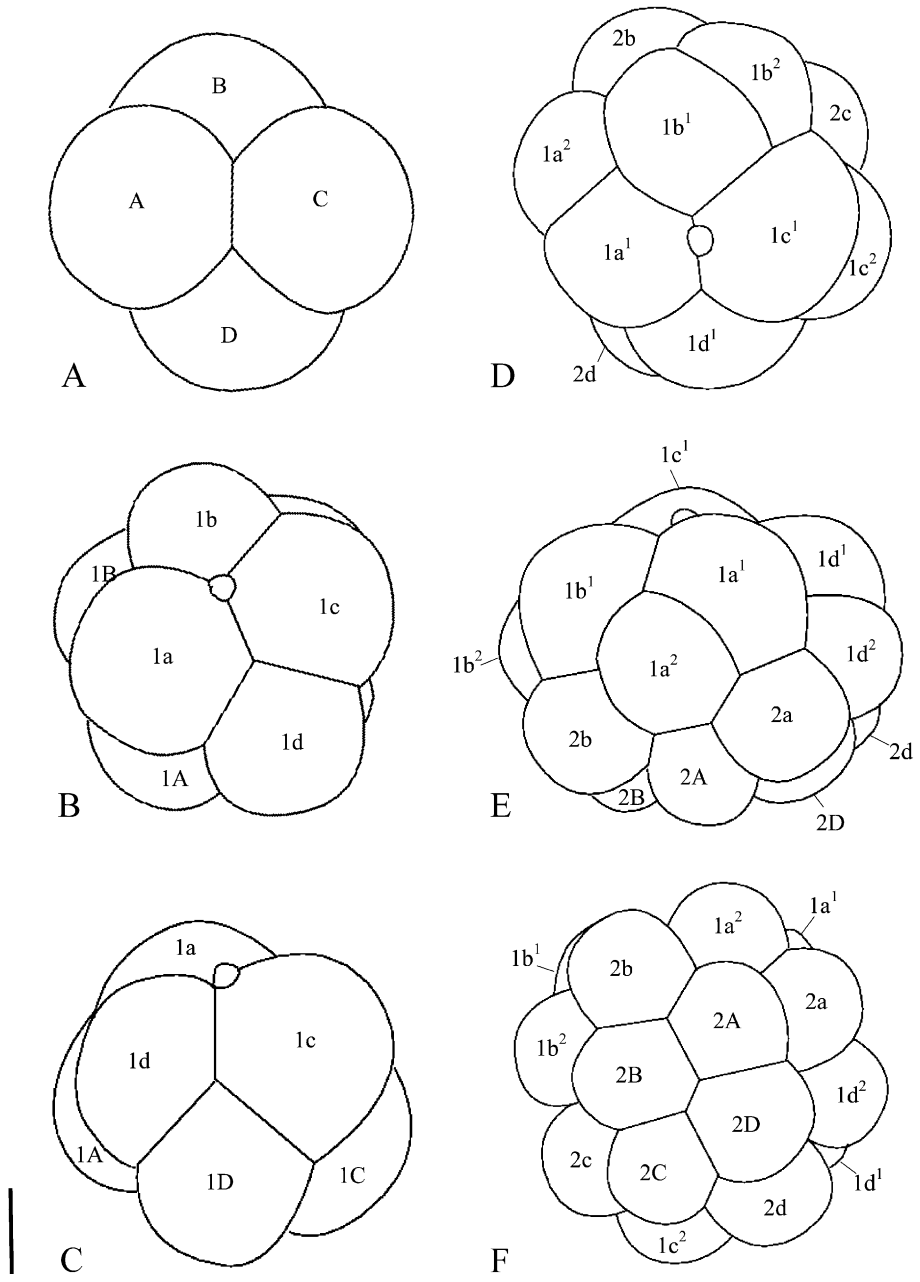

Fig. 1. Cleavage of *Carinoma tremaphoros*: 4- through the 16-cell stage. (A) Animal view of the four-cell stage. Note the conspicuous cross-furrow separating A and C blastomeres. (B) Animal view of eight-cell stage. (C) Lateral view of eight-cell stage. Micromeres 1a-1d are slightly larger than macromeres 1A-1D. (D-F) 16-cell stage. Macromeres 1A–D and first quartet micromeres 1a–1d divide synchronously. Animal progeny of the first quartet micromeres $1a^1$–$1d^1$ are the largest cells in the embryo. (D) Animal view; (E) lateral view; (F) vegetal view. Scale 25 μm.

to cleave normally at the same rate as uninjected controls. The embryos injected with DiI were raised at 24 °C for a period of 48–72 h and observed alive on a Zeiss Axioplan equipped for DIC and fluorescence microscopy. Swimming larvae were partially immobilized by mounting them in a dilute gelatin solution (1–2%) on ice and slightly compressed under a cover slip supported by clay feet. Embryos injected with tetramethylrhodamine were raised for a period of 24–26 h and fixed following the protocol described above for confocal microscopy. Fixed larvae were counterstained with the f-actin binding 488 Alexa Fluor Phalloidin (Molecular Probes, Inc.) to facilitate visualization of the larval morphology, mounted in Vectashield on the poly-L-lysin pretreated slides and viewed on a Nikon E-800 Eclipse microscope with the Bio-Rad Radiance 2100 confocal system equipped with argon-ion and helium-neon lasers. To visualize the red (tetramethylrhodamine) and green (488 Alexa Fluor Phalloidin) labels, helium-neon and argon lasers were set to emit at 543 and 488 nm, respectively.

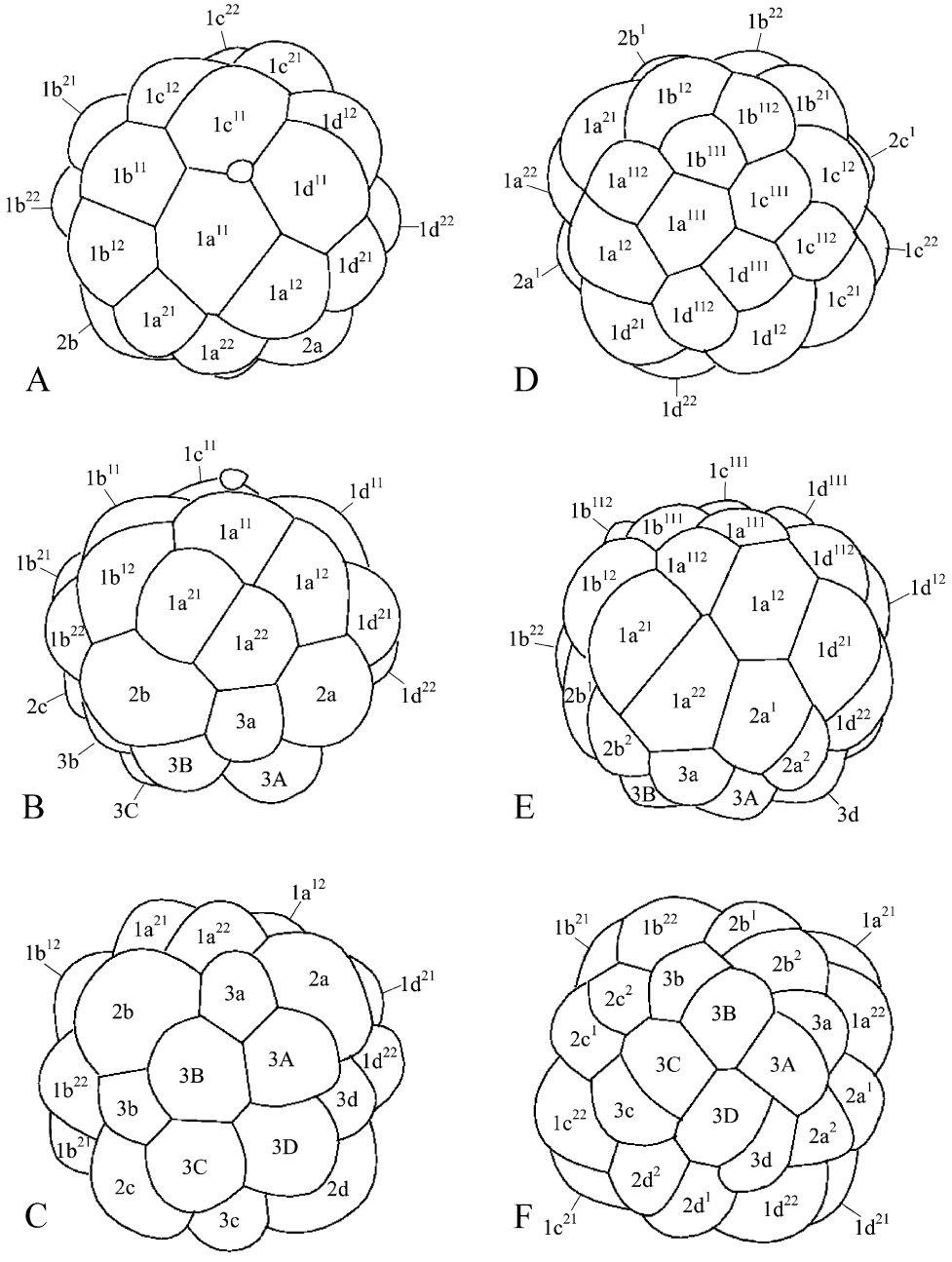

Fig. 2. Cleavage of *Carinoma tremaphoros*: 28- and 36-cell stage. (A–C) 28-cell stage. Cells of the first quartet progeny $1a^1$–$1d^1$ and $1a^2$–$1d^2$ (primary trochoblasts) have divided. The third quartet, 3a–3d, is formed. Division of the second quartet 2a–2d is delayed. (A) Animal view; (B) lateral view; (C) vegetal view. (D–F) 36-cell stage. The apical cells $1a^{11}$–$1d^{11}$ have divided forming the apical rosette cells $1a^{111}$–$1d^{111}$ and the peripheral rosette cells $1a^{112}$–$1d^{112}$, and second quartet 2a–2d have divided. (D) Animal view; (E) lateral view; (F) vegetal view. Scale 25 μm.

Illustrations and nomenclature

Figs. 1–4 represent tracings of the cleavage stages of *C. tremaphoros* from 4- to 64-cell stages made from the confocal projections of the whole mount preparations (Figs. 5, 6). In labeling individual cells we followed broadly accepted nomenclature of spiral cleavage (Wilson, 1892; modified by Child, 1900). This nomenclature has the following essential components: (1) quadrants are labeled as A, B, C and D; (2) quartets are labeled as first, second,

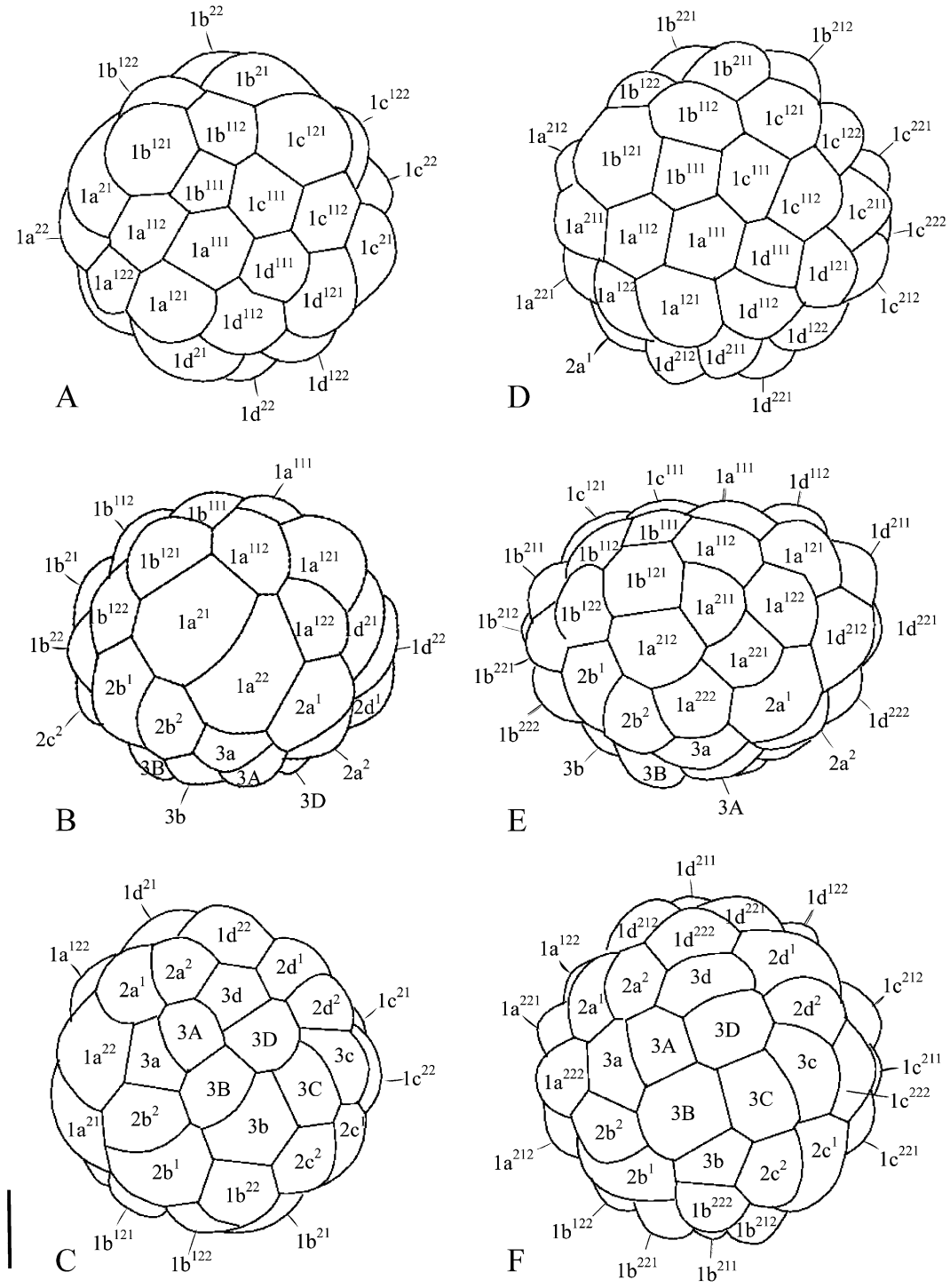

Fig. 3. Cleavage of *Carinoma tremaphoros*: 40- and 48-cell stage. (A–C) 40-cell stage. Progenitors of the molluscan cross $1a^{12}$–$1d^{12}$ have divided. (A) Animal view; (B) Lateral view; (C) Vegetal view. (D–F) 48-cell stage. Trochoblasts $1a^{21}$–$1d^{21}$and a^{22}–$1d^{22}$ have divided forming 16 primary trochoblasts $1a^{211}$–$1d^{211}$, $1a^{212}$–$1d^{212}$, $1a^{221}$–$1d^{221}$ and $1a^{222}$–$1d^{222}$, which undergo cleavage arrest. (D) Animal view; (E) lateral view; (F) vegetal view. Scale 25 μm.

third and fourth; (3) micromeres and macromeres are labeled with lower- and uppercase letters, respectively; and (4) lineages downstream of the starting nodes are labeled with superscripts. Because the cleavage is equal the denomination of the quadrants on (Figs. 1–4, 7 and 14) is not definitive. The letter "Q" is used when referring to all the cells (A, B, C and D) of a particular quartet. The A and C quadrants are the two lateral quadrants that form

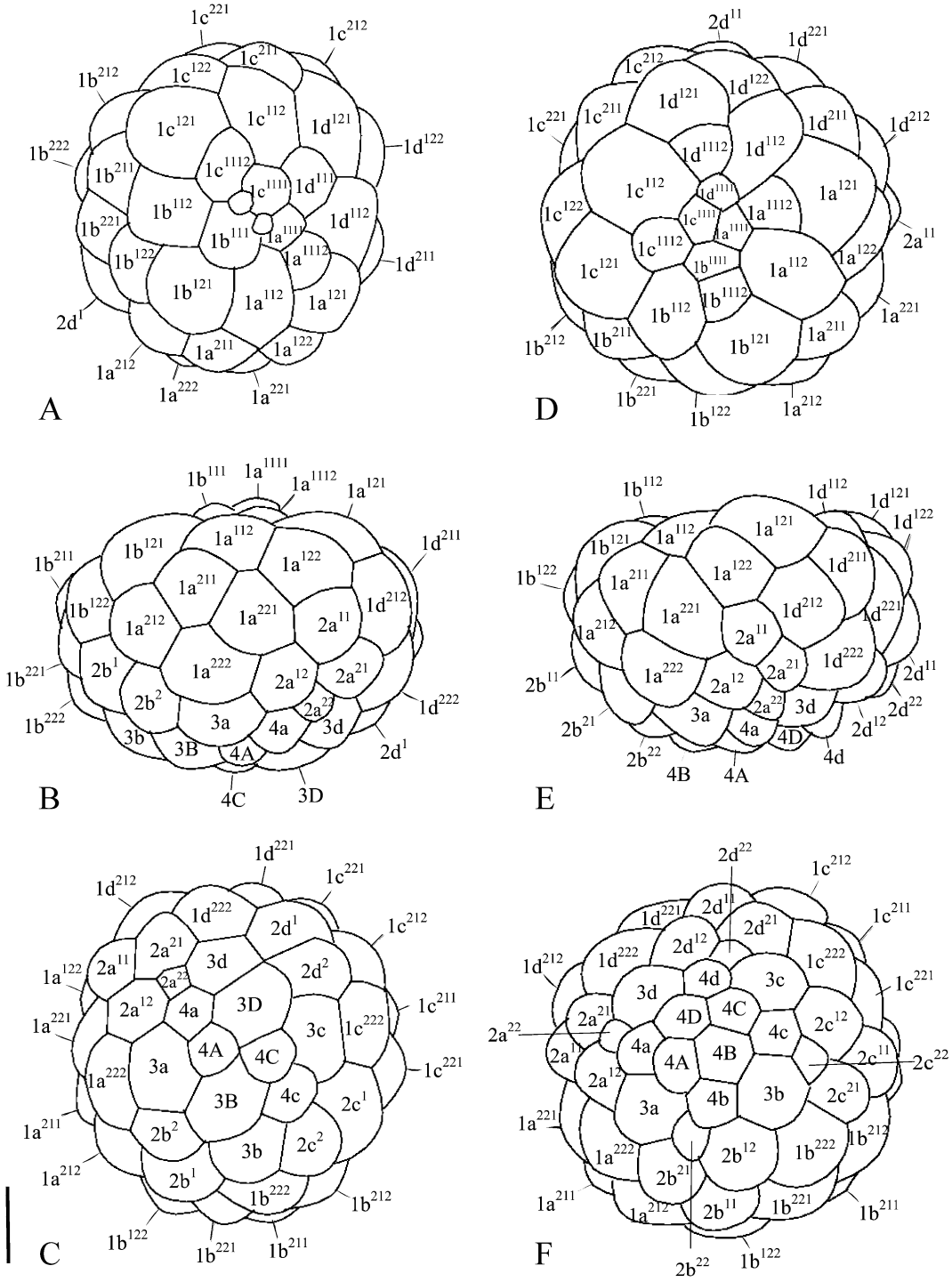

Fig. 4. Cleavage of *Carinoma tremaphoros*: 54- and 64-cell stage. (A–C) 54-cell stage. Two apical rosette cells, $1a^{111}$ and $1c^{111}$, undergone seventh division. Second quartet micromere progeny of the A quadrant, $2a^{1}$ and $2a^{2}$, have undergone 6th division. Two fourth quartet micromeres 4a and 4c have formed. (A) Animal view; (B) lateral view; (C) vegetal view. (D–F) 64-cell stage. The embryo becomes flattened along the animal–vegetal axis, with the animal pole "sinking". Apical rosette cells located at the bottom of the apical invagination finished seventh division. Second quartet progeny and the macromeres finished sixth division. Division of the third quartet micromeres 3a–3d is delayed. (D) Animal view; (E) Lateral view; (F) Vegetal view. Scale 25 μm.

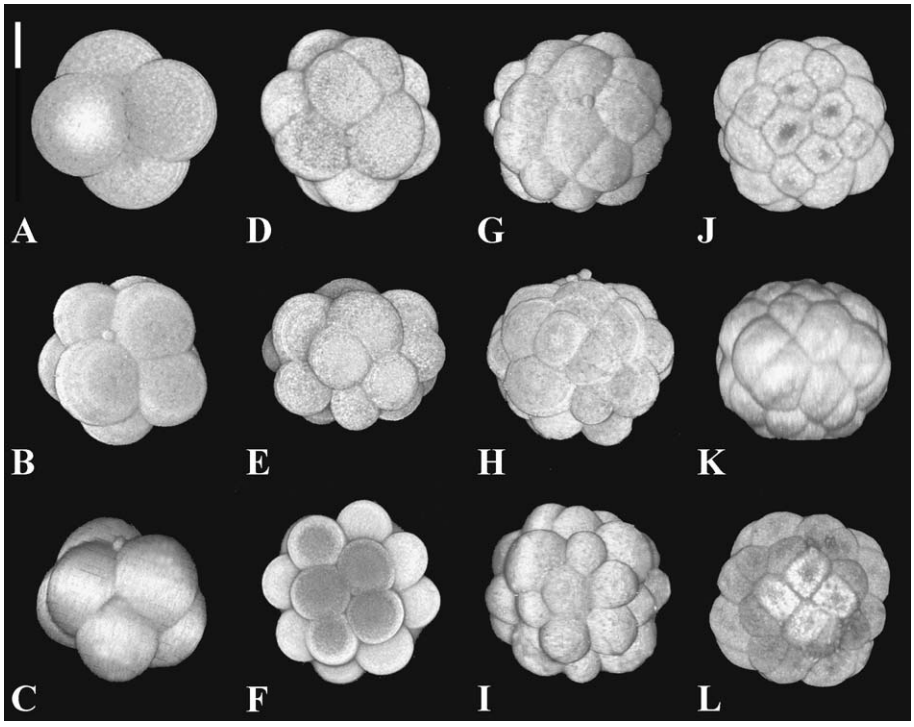

Fig. 5. Confocal projections of whole-mount preparations of *Carinoma tremaphoros* embryos: 4- through 36-cell stage. (A) Animal view of the four-cell stage (B) Animal view of the eight-cell stage. (C) Lateral view of the eight-cell stage. (D–F) 16-cell stage. (D) Animal view; (E) Lateral view; (F) Vegetal view. (G–I) 28-cell stage. (G) Animal view; (H) lateral view; (I) vegetal view. (J–L) 36-cell stage. (J) Animal view; (K) lateral view; (L) vegetal view. Scale 25 μm.

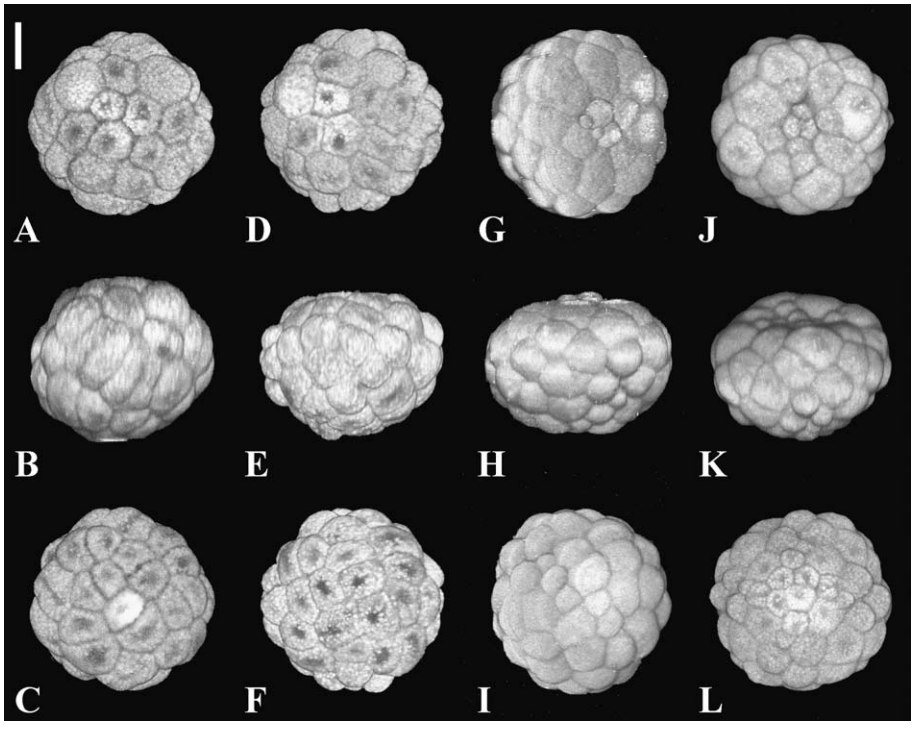

Fig. 6. Confocal projections of whole-mount preparations of *Carinoma tremaphoros* embryos: 40- through 64-cell stage. (A–C) 40-cell stage. (A) Animal view; (B) lateral view; (C) vegetal view. (D–F) 48-cell stage. (D) Animal view; (E) lateral view; (F) vegetal view. (G–I) 54-cell stage. (G) Animal view; (H) lateral view; (I) vegetal view. (J–L) 64-cell stage. (J) Animal view; (K) lateral view; (L) vegetal view. Scale 25 μm.

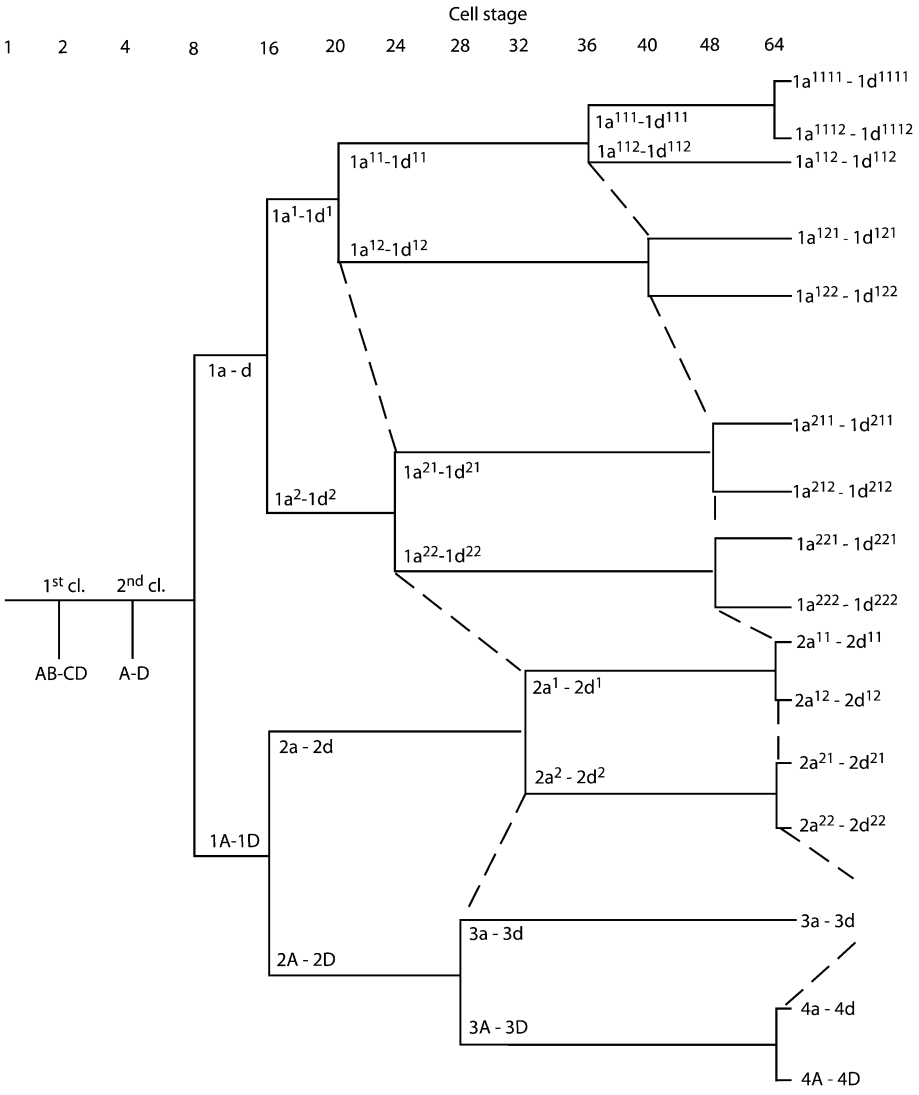

Fig. 7. Diagram of *Carinoma tremaphoros* cell lineage showing relative timing of quartet divisions. Dashed lines illustrate temporal shifts in the division of the cells of the same "generation". Note relative retardation in the division of second and third micromere quartets compared to their macromeres.

a cross-furrow at the animal pole. The B and D quadrants are the median quadrants that define the dorso-ventral axis and form a cross-furrow on the vegetal pole. Figs. 9, 10 and 12, illustrating labeling domains, were drawn from the confocal projections of whole mount larvae counter-stained with phalloidin to visualize the cell borders (Figs. 8, 11). We refer to all taxa possessing spiral cleavage as "spiralian taxa" or "spiralians" (polyclad turbellarians, mollusks, annelids, echiurids, sipunculids, nemerteans and entoprocts).

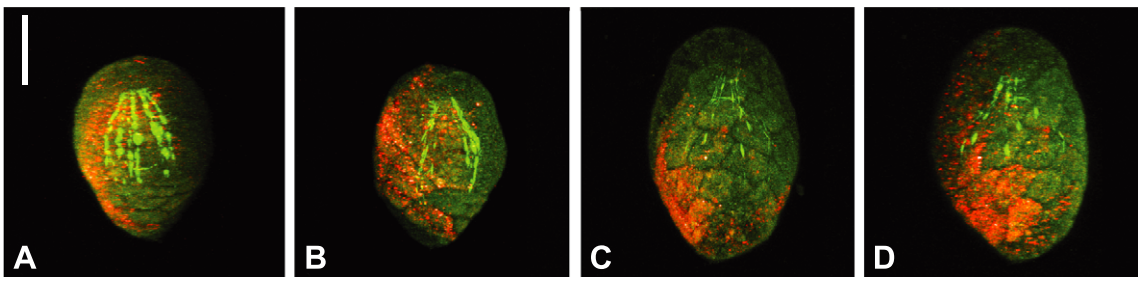

Fig. 8. Confocal projections of *Carinoma tremaphoros* larvae (24–26 h) injected with lysinated tetramethylrhodamine at two-cell stage. (A) AB pattern, dorsal view; (B) AB pattern, left view; (C) CD pattern, ventral view; (D) CD pattern, right view. Scale 50 μm.

Results

Cleavage and early development

C. tremaphoros exhibits equal holoblastic spiral cleavage. Eggs are 90–110 μm in diameter, whitish and moderately opaque, surrounded by a very thin (2.5 μm) and highly transparent egg chorion 160–170 μm in diameter. Oocytes are densely packed inside the ovaries, so that when released, they are highly compressed and have the appearance of hollow hemispheres. Upon contact with seawater, eggs round up and undergo germinal vesicle breakdown in about 10–20 min. The first polar body forms approximately 10 min after fertilization, followed by the second polar body approximately 10 min later. Occasionally, one of the polar bodies divides so that two or three polar bodies can be distinguished at the animal pole of the egg. First, cleavage begins approximately 40 min after fertilization, producing two equal-sized blastomeres, which are rounded and in the process of division are connected by a very narrow cytoplasmic bridge. In a few minutes, the embryo becomes compact and soon divides into four cells. Intervals between the first few divisions are approximately 20 min (Table 1). Second cleavage is slightly spiral and sinistral: spindles are reclined with respect to the animal vegetal axis of the embryo and the two "animal" daughter cells are shifted counterclockwise with respect to "vegetal" cells when viewed from the animal pole. Each pair of animal and vegetal blastomeres at the four-cell stage is separated by the cross-furrow (Figs. 1A–B, 5A–B). The two cross-furrows remain distinguishable even after compacting of blastomeres. Third cleavage is dextral and unequal: animal "micromeres" are, in most cases, slightly larger than vegetal "macromeres" (Figs. 1C, 5C). There is some variability among egg batches: in some, the size difference between first quartet micromeres and macromeres is very distinct, in others, they are almost indistinguishable. The next division of the micromeres is asymmetric, with the largest cells at the 16-cell stage being the most animal cells ($1a^1$–$1d^1$) (Figs. 1D–E, 5D–E).

Micromeres of the 1st quartet tend to begin division 1–5 min earlier than macromeres. Subsequent divisions are asynchronous between the quartets. After the 16-cell stage, intervals between divisions become longer (Table 1). The transition from 16 to 32 cells occurs via three short stages: 20 (1 min), 24 (4–6 min) and 28 (2 min) cells (Figs. 2, 5). Cleavage, generally, starts with cells located at the animal pole, progressing toward cells at the vegetal pole, with the exception of the macromeres 2A–2D and 3A–3D, which divide earlier than their sister cells (2a–2d and 3a–3d, correspondingly) (Figs. 2B–C, 4B–C, E–F, 5H–I, 6H–I, K–L). At the 64-cell stage, the animal pole becomes flattened and slightly invaginated, with micromeres $1a^{1111}$–$1d^{1111}$ (animal daughters of the apical rosette cells) situated at the bottom of the depression (Figs. 4D–E, 6J–K); however, internally, the embryo remains hollow with animal micromeres and the macromeres separated by the cleavage cavity. The earliest signs of ciliation appear 4 h after fertilization. The lateral surface of the embryo appears to become ciliated first, whereas ciliation of the apical and vegetal regions is delayed. Gastrulation begins at 5 h when the embryo is uniformly ciliated and rotates within the egg chorion.

Table 1
Timetable of early development of *Carinoma tremaphoros*

Stage	Time (h:min at 24 °C)
Fertilization	00:00
1st polar body formation	00:10
2nd polar body formation	00:20
2 cells	00:40
4 cells	01:00
8 cells	01:20
16 cells	01:40
32 cells	02:05
64 cells	03:00
First ciliation	04:00
Gastrulation	05:00
Hatching	05:30

Approximate times are calculated as average of five different batches of embryos.

Larval development

Uniformly ciliated spherical gastrulae possessing a long apical tuft hatch at approximately 5.5 h after fertilization. After hatching, larvae gradually elongate and the blastopore shifts to the ventral side due to proliferation of the cells of the dorsal surface. Maslakova et al. (in review) demonstrated that at this stage the larval surface is covered by the 40 large squamous cells except for the apical and posterior poles. At 23–24 h, actively swimming larvae measure about 150 μm in length, possess a single ventrolateral eye, well-developed apical tuft and small caudal cirrus at the posterior end. At this stage, larvae begin to develop musculature and become contractile. Cells of apical and posterior regions divide further, while the 40 large ectodermal cells are cleavage-arrested and form a pre-oral belt, skewed with respect to the antero-posterior axis of the larva (Maslakova et al., in review). These cells can be seen on the confocal projections of larvae, labeled at 16-cell stage (Fig. 11). We also included the cell outlines of these large ectodermal cells on the diagrams of cell lineage (Figs. 9, 10, 12). Based on it's morphology and position, Maslakova and Norenburg (2001) and Maslakova et al. (in review) suggested that this belt corresponds to the prototroch of other Eutrochozoa such as mollusks, annelids, echiurids and sipunculids.

Cell labeling at the two-cell stage

Only two different complimentary patterns were observed as result of the series of injections at the two-cell

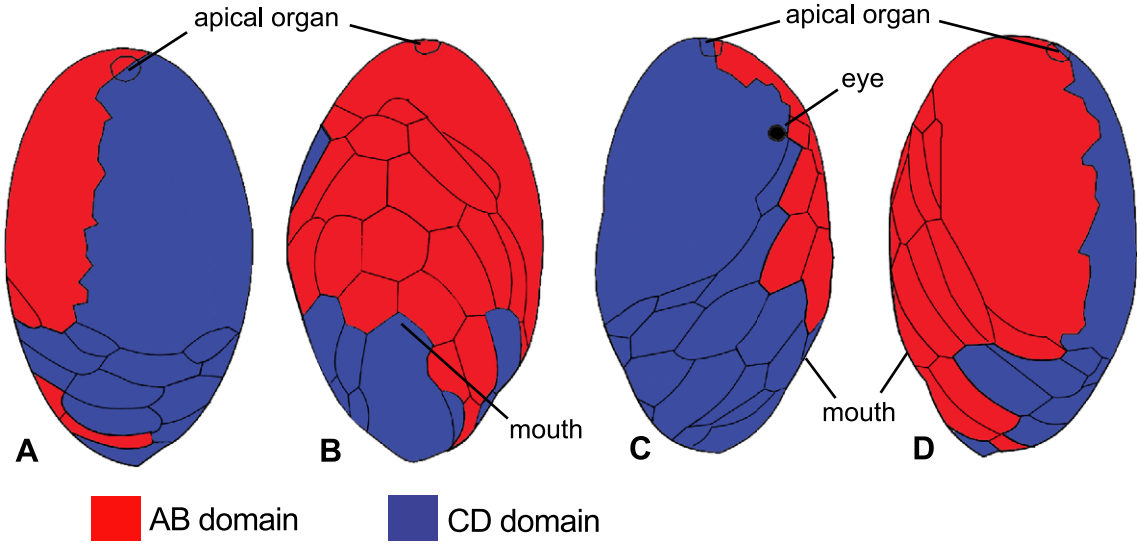

Fig. 9. Labeling domains of AB and CD cells in 25 h *Carinoma tremaphoros* larvae). (A) Dorsal view; (B) a slightly oblique ventral view (ventral–ventral-left); (C) right view; (D) a slightly oblique left view (left-anterior).

stage. Labeled ectodermal domains included an anterior ventral-left pattern and a complementary posterior dorsal-right pattern, called AB and CD, respectively, due to their spatial similarity to domains in other eutrochozoan embryos (Figs. 8A–D, 9A–D). The AB blastomere produces ventral ectoderm anterior to the mouth, while ventral ectoderm posterior to the mouth is derived from the CD cell. Ectoderm of the left side is almost entirely produced by the AB-cell, with the exception of the a little "flap" of CD origin posterior to the mouth (Figs. 8A–B, 9A–B, D). Results of the 16-cell stage labeling reveal that this "flap" corresponds to the four large cells composing dorsal part of the pre-oral belt of cells, which Maslakova et al. (in review) identify as a prototroch, derived from the lineage corresponding to the primary trochoblast lineage in other spiralians—$1d^2$ (Figs. 11H, 12A–B, D). The CD blastomere produces an exact compliment to AB pattern and includes most of the ectoderm posterior to the mouth, except the narrow "flap" of AB origin, reaching over to the dorsal side posterior to the progeny of $1d^2$ cell (Figs. 8A–D, 9A–B, D). This AB "flap" corresponds to the three prototroch cells (Maslakova et al., in review) derived from the second quartet micromere 2a (lineage that corresponds to the secondary trochoblasts in other spiralians) (Figs. 11I, 12A–B, D). The CD cell also produces ectoderm of the right side and includes the only larval eye, located anteriorly on the ventral side to the right of the midline (Figs. 8C–D, 9A–B, D). Both AB and CD domains contribute to the apical organ and meet ventrally at the mouth (former blastopore). The number of cases displaying each of these labeled domains is recorded in Table 2. In each case, the labeled domain included a portion of the oesophagus and gut; however, the distribution of labeled cells in deeper structures (mesoderm and endoderm) is somewhat obscured by the overlaying ectodermal domains and will not be described in detail here. No other patterns were observed. Therefore, the first cleavage plane assumes a consistent orientation relative to the plane of bilateral symmetry of the larva.

Cell labeling at the four-cell stage

Labeling at the four-cell stage resulted in four distinct patterns that represented subsets of the AB and CD domains obtained in the two-cell stage labeling experiments. Observed labeled ectodermal domains included a left (A), anterior ventral (B) and roughly mid-dorsal (D) patterns (Figs. 10A–D). Quadrant A corresponds to the left part of the AB domain described above, while pattern B forms a complimentary region of AB domain and includes the ventral ectoderm anterior to the mouth. Quadrant D corresponds to the dorsal and ventral part of the CD domain and occupies mid-dorsal region, posterior end and mid-ventral region posterior to the mouth (blastopore). Although no C cases were observed in the four-cell stage labeling experiments (Table 2), we extrapolated it as a complimentary domain to A + B + D. This was confirmed by the labeling experiments at the 8- and 16-cell stages: the same ectodermal C domain was obtained by the addition of the 1c and 1C domains (Table 2, Fig. 10) or $1c^1$, $1c^2$ and 2c (Table 2, Figs. 11, 12). The C quadrant, therefore, corresponds to the right side of the CD pattern and includes the single larval eye (Fig. 10C). All four domains included part of the apical organ, a portion of the oesophagus and the gut (internal labeling, obscured by the ectodermal patterns, is not shown).

First-quartet micromeres and their progeny

Better resolution of the nature of the spiralian cleavage pattern can be made by observing the fates of the animal

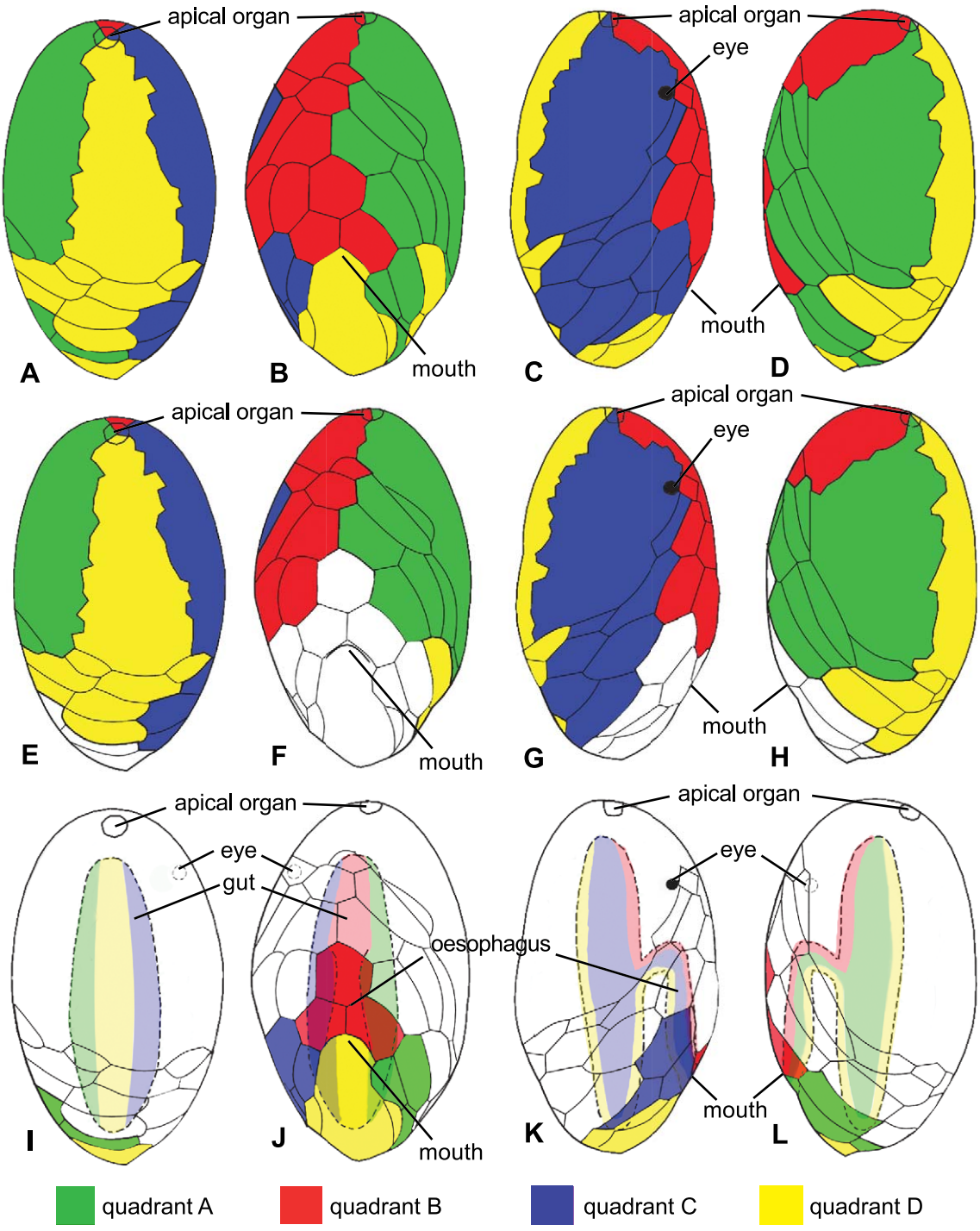

Fig. 10. Labeling domains in 25 h *Carinoma tremaphoros* larvae. (A–D) Labeling domains of the quadrants A, B, C and D. (E–H) First quartet micromere domains. (I–L) First quartet macromere domains. (A, H, I) Dorsal view; (B, J, F) a slightly oblique ventral view (ventral–ventral-left); (C, K, G) right view; (D, L, H) a slightly oblique left view (left-anterior). Although no "C" pattern cases were observed in the four-cell stage labeling experiments (Table 2), we extrapolated it as a complimentary domain to "A"+"B"+"D". This was confirmed by the labeling experiments at the 8- and 16-cell stage: "C" domain can be obtained by the addition of the "1c" and "1C" or "$1c^1$", "$1c^2$", and "2c" domains.

micromeres and their corresponding vegetal macromeres. Individual micromeres were injected at the 8- and 16-cell stage. In case of the eight-cell stage labeling, four distinct ectodermal domains, identified as 1a, 1b, 1c and 1d, were observed. Injected embryos were sorted according to whether the labeled cell was a cross-furrow or a non-cross-furrow micromere (Fig. 1B, cross-furrow micromeres labeled 1a and 1c, non-cross-furrow micromeres labeled 1d and 1b). Two labeling patterns were obtained in each case. When one cross-furrow micromere was injected, the labeling pattern corre-

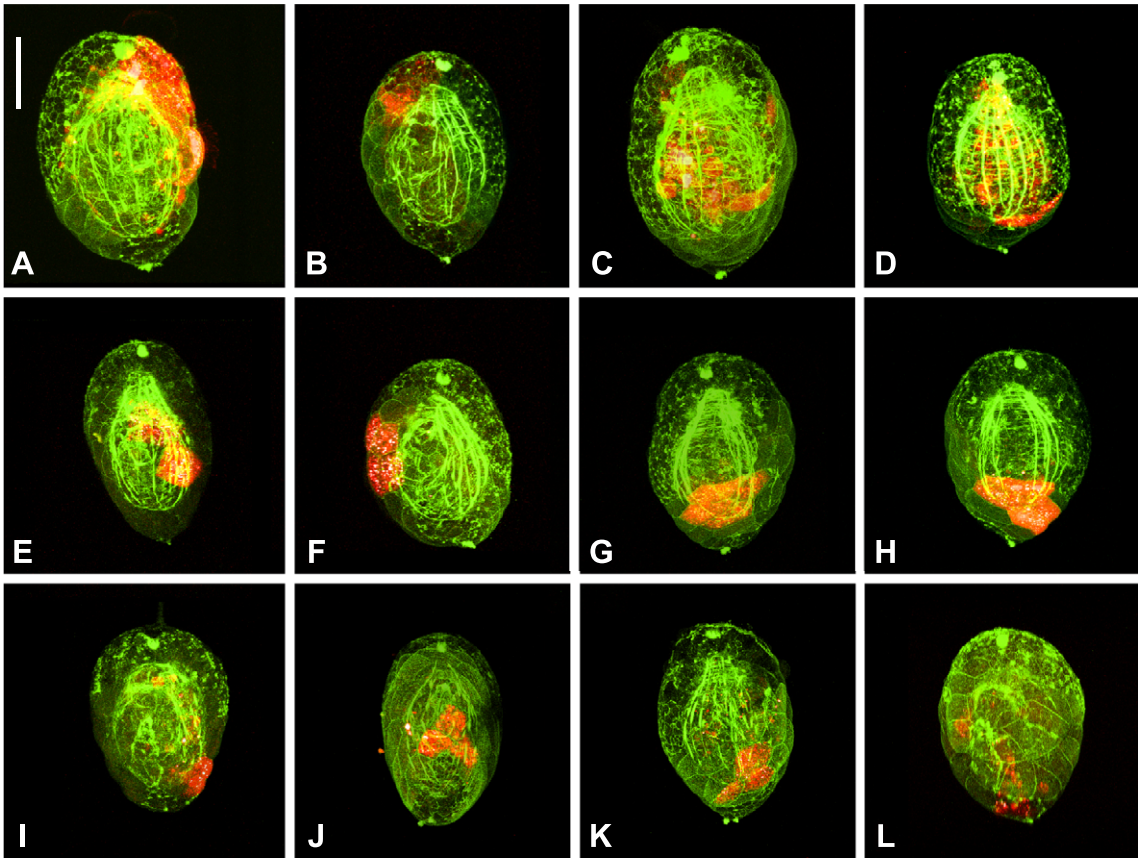

Fig. 11. Confocal projections of *Carinoma tremaphoros* larvae (24–26 h) injected with lysinated tetramethylrhodamine at the 16-cell stage. (A–D) Animal progeny of the first quartet micromeres: (A) $1a^1$, ventral view; (B) $1b^1$, left-ventral view; (C) $1c^1$, right view; (D) $1d^1$, dorsal view. (E–H) Vegetal progeny of the first quartet micromeres: (E) $1a^2$, ventral view; (F) $1b^2$, ventral-right view; (G) $1c^2$, right view; (H) $1d^2$, left view. (I–L) Second quartet micromeres: (I) 2a, ventral view; (J) 2b, ventral view; (K) 2c, right view; (L) 2d, ventral-left view. Scale 50 μm.

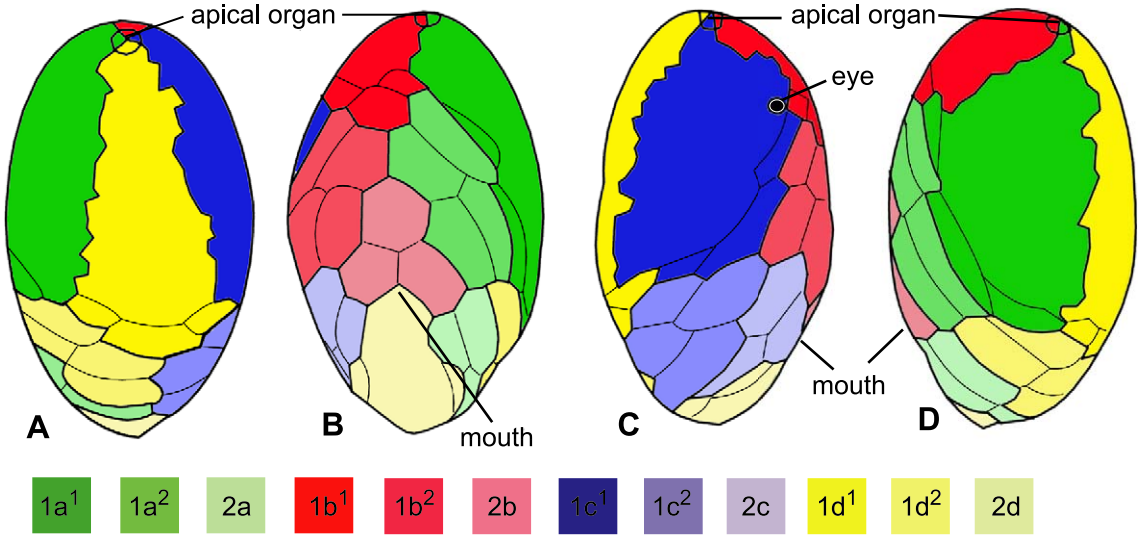

Fig. 12. Summary diagram of micromere ($1q^1$, $1q^2$ and 2q) domains in the 25 h old *Carinoma tremaphoros* larvae. Similar to other Eutrochozoa, *C. tremaphoros* possesses a prototroch, composed of 40 cells (16 trochoblasts derived from the $1q^2$ lineage, 12 trochoblasts derived from the $1q^1$ lineage and 12 trochoblasts derived from the 2^{nd} quartet micromeres). (A) Dorsal view; (B) a slightly oblique ventral view (ventral–ventral-left); (C) right view; (D) a slightly oblique left view (left-anterior).

Table 2
Occurrence of cell-labeling patterns in *Carinoma tremaphoros* larvae (24–78 h)

Injected cell	Pattern observed	Number of cases observed
Two-cell stage blastomere	AB	25
(46 cases examined)	CD	21
Four-cell stage blastomere	A	5
(9 cases examined)	B	3
	C	0
	D	1
First quartet micromere	1a	6
either cross-furrow or	1b	16
non-cross-furrow	1c	7
(38 cases examined)	1d	9
First quartet cross-furrow	1a	7
micromere (16 cases examined)	1c	9
First quartet non-cross-furrow	1b	18
micromere (30 cases examined)	1d	12
First quartet cross-furrow	1B	8
macromere (17 cases examined)	1D	9
First quartet non-cross-furrow	1A	9
macromere (21 cases examined)	1C	12
Animal progeny of the first	$1a^1$	5
quartet micromere	$1b^1$	3
(24 cases examined)	$1c^1$	10
	$1d^1$	6
Vegetal progeny of the first	$1a^2$	9
quartet micromere	$1b^2$	11
(40 cases examined)	$1c^2$	14
	$1d^2$	6
Second quartet micromere	2a	2
(12 cases examined)	2b	4
	2c	5
	2d	1

sponded to either 1a or 1c. Injected non-cross-furrow cells produced the other two patterns—1b and 1d (Table 2). These domains represent clear subsets of the two- and four-cell patterns and consist of the corresponding domains of the 16-cell stage labeling (Figs. 10E–H, 11A–H). Analysis of the labeled domains reveals that first quartet micromeres contribute to the majority of the larval ectoderm. Analysis of the 16-cell stage labeling domains reveals that animal daughter of each of the first quartet micromeres ($1q^1$) contributes to the apical organ, pre-trochal ectoderm of the corresponding domain at the four- and eight-cell stage and three prototroch cells (Figs. 11A–D, 12A–D). The animal daughter of the first quartet micromere in C quadrant ($1c^1$) produces the single larval eye situated ventrally anterior to the prototroch to the right off the midline. As in other Eutrochozoans, vegetal daughter of each of the first quartet micromeres ($1q^2$) contributes to the four central cells of the prototroch—called the primary trochoblasts (Figs. 11E–H, 12A–D).

First-quartet macromeres and their progeny

First quartet macromeres (1Q) and second quartet micromeres (2q) were injected at the 8- and 16-cell stage, respectively (Table 2). First quartet macromeres produce four distinct labeling domains identified as 1A, 1B, 1C and 1D. These domains represent clear subsets of the two- and four-cell patterns and their ectodermal components correspond to second quartet micromere domains (Figs. 10I–L, 11I–L, 12A–D). The cross-furrow at the vegetal pole allows the distinction to be made between cross-furrow and non-cross-furrow blastomeres. Two distinct patterns are obtained in each case (Table 2). Injected cross-furrow macromeres produce 1B and 1D patterns, while non-cross-furrow macromeres produce 1A and 1C domains. The 1D domain includes three dorsal prototroch cells, all the post-trochal ectoderm, the floor of the oesophagus and part of the gut, where all the ectodermal contribution is from the second quartet micromere–2d (Figs. 10I–L, 11L, 12A–D). The 1B pattern includes three ventral prototroch cells (derived from the second quartet micromere 2b, corresponding to the secondary trochoblasts in other spiralians), the roof of the oesophagus and part of the gut (Figs. 10J–L, 11J, 12B, D). The 1A labeling domain includes three prototroch cells on the left side (derived from the 2a, corresponding to the secondary trochoblast lineage), the left side of the oesophagus and left side of the gut (Figs. 10I, J–L, 11I, 12A–B, D). The 1C domain includes three prototroch cells on the right side (derived from the 2c, corresponding to the secondary trochoblasts of other spiralians), right side of the oesophagus and right side of the gut (Figs. 10J–K, 11K, 12B, C). Injection of individual 2Q macromeres generated internal descendants and is not described here.

Discussion

Size and timing of cell division

All nemerteans thus described possess equal spiral cleavage, such that there is no size difference between the quadrants at the four-cell stage. Cleavage beyond the 16-cell stage had been traced in six nemertean species: four heteronemerteans *C. lacteus* (Wilson, 1903), *Cerebratulus marginatus* (Zeleny, 1904), *Lineus torquatus* (Iwata, 1957) and *Lineus ruber* (Schmidt, 1962, 1964) and two hoplonemerteans—*Emplectonema gracile* (Delsman, 1915) and *Malacobdella grossa* (Hammarsten, 1918). Here, we present the first description of a palaeonemertean cleavage program. Subtle differences between the cleavage patterns of various nemertean species in relative size and timing of the formation and division of different micromere and macromere quartets exist. As in most nemerteans and sipunculids, but unlike the typical spiral cleavage of annelids and mollusks, the first quartet of micromeres of *C. tremaphoros* is slightly larger than the macromeres (Friedrich, 1979). A survey of the early cleavage of several sipunculid species reveals that the relative size of micromeres and macromeres at the eight-cell stage is related to

the yolk content of the egg. Micromeres exceed the macromers in size only in eggs with a high yolk content and in which the development is lecithotrophic. Those species with microlecithal eggs have micromeres equal to or smaller than the macromeres. This size difference is also reflected in the enormous yolk-laden cells of the sipunculid prototroch (Pilger, 1997; Rice, 1985). The trend is opposite in mollusks, echiurids and annelids: in species with microlecithal eggs, eight equal-sized blastomeres are formed, while in species with yolky eggs, the macromeres are larger and more yolky than the micromeres (Casteel, 1904; Collier, 1997; Conklin, 1897; Gould-Somero, 1975; Meisenheimer, 1900; Pilger, 1997; Schroeder and Hermans, 1975; Wierzejski, 1905). Nemertean egg sizes vary from 50 μm to 2.5 mm (Friedrich, 1979; Henry and Martindale, 1997 and references therein). Relative sizes of blastomeres at the eight-cell stage had been recorded for a small fraction of species for which egg size is known (Delsman, 1915; Hammarsten, 1918; Iwata, 1957, 1958, 1960; Maslakova and Malakhov, 1999; Reinhardt, 1941; Schmidt, 1962; Wilson, 1903; Zeleny, 1904; SAM personal observation). In all nemertean species, without regard to the egg size, animal micromeres are larger or equal in size to vegetal macromeres. The only exceptions in which the micromeres are reportedly smaller than the macromeres are the palaeonemertean *Tubulanus notatus* (Dawydoff, 1928, cited from Friedrich, 1979) and the hoplonemerteans *Tetrastemma vermiculus* and *Drepanophorus spectabilis* (Lebedinsky, 1898). It would be prudent to reexamine these cases.

In nemerteans, cleavage generally proceeds from the animal tier of cells to the vegetal pole, with the animal—most micromeres dividing first and the macromeres dividing last. However, there are several deviations from this rule. The second and third macromere quartets of *C. tremaphoros* divide before their corresponding quartet of micromeres (Figs. 2, 4–7). This characteristic relative retardation of the second- and third-quartet micromere division is also found in a heteronemertean *L. torquatus* (Iwata, 1957), and Wilson (1903) and Zeleny (1904) noticed similar retardation of the second-quartet micromere division in the heteronemerteans *C. lacteus* and *C. marginatus*. It is not known whether third-quartet micromere division in these species is delayed. In contrast, the hoplonemerteans, *E. gracile* (Delsman, 1915), *M. grossa* (Hammarsten, 1918), *Tetrastemma worki* (SAM personal observation), and *Amphiporus ochraceus* (SAM personal observation) and the heteronemertean *L. ruber* (Schmidt, 1962, 1964) do not show a delay in the vegetal cells. Some of these changes in timing of cell division correlate with the relative size of the blastomeres: larger cells divide faster than their smaller sisters, and animal daughters are typically larger than the vegetal daughters in the first three or four divisions in nemertean embryos (Delsman, 1915; Hammarsten, 1918; present study Figs. 1, 2). However, not always can such a generalization be made. This means that although cell size is often a good predictor of the cell division timing, it is not universal.

The timing of cell division (e.g., relative timing of formation of the individual blastomeres or quartets with respect to the total number of cells in the embryo) has been shown to reflect phylogenetic relationships among gastropod mollusks—a group in which the information on early cleavage can be compiled for a large number of species (Guralnick and Lindberg, 2001; van den Biggelaar and Haszprunar, 1996). However, lack of detailed information on early development of most spiralians and, particularly, such understudied groups as Nemertea, Sipunculida, Echiurida and Entoprocta does not yet allow a robust reconstruction of the interphyletic relationships.

Farewell to molluscan and annelid cross

The presence of the apical cross-like pattern, formed by the progeny of the first and second quartet micromeres in some eutrochozoans received attention by many embryologists (Conklin, 1897; Gerould, 1906; Mead, 1897; Rice, 1985; Scheltema, 1993; Wilson, 1892). Two major patterns are distinguished: the so-called molluscan cross (described in some gastropod mollusks and one sipunculid) and the annelid cross (described in some annelids and one echiuran). The arms of the molluscan cross are formed by the progeny of cells $1a^{12}$–$1d^{12}$ (Fig. 13, in yellow). The animal daughters of second quartet micromeres ($2a^{1}$–$2d^{1}$) form the tips of the cross (Fig. 13, in green). The first quartet derivatives, $1a^{112}$–$1d^{112}$ (called the peripheral rosette cells), lie between the arms of the molluscan cross and form arms of the annelid cross (Fig. 13, in blue). Nemerteans reportedly have neither a molluscan nor an annelid cross.

The presence of the annelid or molluscan cross has been long considered an important indicator of inter-phyletic relationships. For example, Pilger (1997) suggests that presence of annelid cross in echiurans supports a close phyletic relationship with annelids. Scheltema (1993) argued that the shared presence of a molluscan cross is indicative of close phylogenetic affinities of Mollusca and Sipunculida. Rice (1985), on the other hand, concluded that Sipunculida is a primitive group derived from the annelidan–molluscan stem and closely related to the common ancestor of annelids and mollusks. Acknowledging its possible phylogenetic significance, we have compared our detailed observations of the cleavage program of a palaeonemertean to the apical cleavage mosaic across a range of eutrochozoan taxa, in which the cleavage is well documented: to another nemertean (Figs. 13A–B), one sipunculid (Fig. 13C), six mollusks (Figs. 13D–I) and three annelids (Figs. 13J–L). To facilitate identification, homologous cells are shown in the same color: apical rosette cells—red, annelid cross—blue, molluscan cross—yellow and tips of the molluscan cross—green (Fig. 13).

The molluscan cross is formed when the cells $1a^{12}$–$1d^{12}$ undergo division in which their daughter cells $1a^{121}$–$1d^{121}$

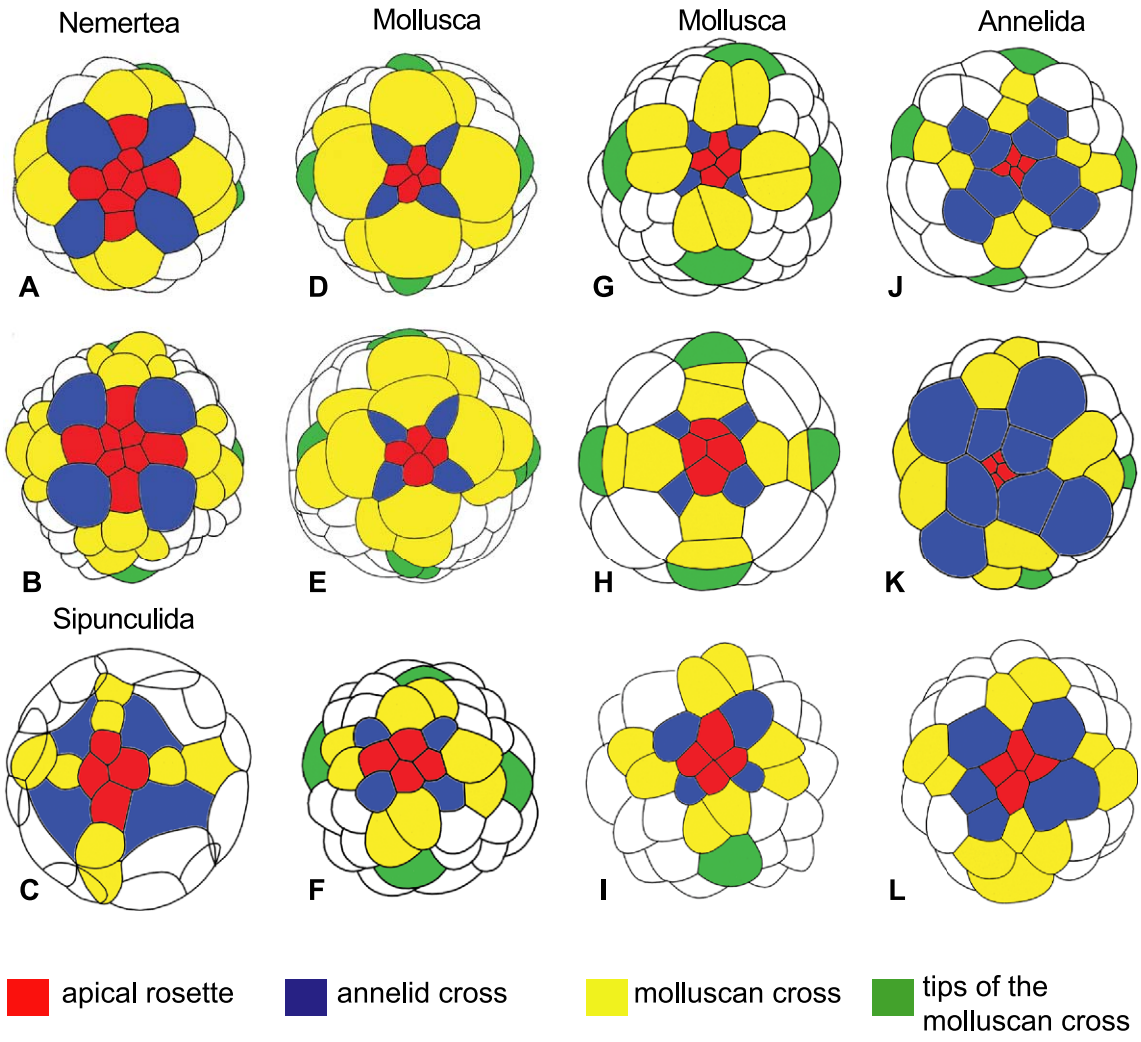

Fig. 13. Apical cell mosaic in various Eutrochozoa. Apical rosette cells $1a^{111}-1d^{111}$ and their progeny are red. Peripheral rosette cells $1a^{112}-1d^{112}$ and their progeny which form the annelid cross are blue. Cells of the molluscan cross $1a^{121}-1d^{121}$, $1a^{122}-1d^{122}$ and their progeny are yellow. Tip cells of the molluscan cross $2a^{11}-2a^{11}$ are green (only shown where they are identified). (A–B) Nemertea: (A) palaeonemertea (*Carinoma tremaphoros*) 64-cell stage; (B) hoplonemertea (*Emplectonema gracile*, after Delsman, 1915, pl. VIII, Fig. 27) 84-cell stage. (C) Sipunculida (*Golfingia vulgaris*, after Gerould, 1906, p.99, Fig. D.) 48-cell stage. (D–I) Mollusca: (D) polyplacophora (*Stenoplax heathiana*) transition from 55- to 63-cell stage (after Heath, 1899, pl. 32, Fig. 17); (E) polyplacophora (*Stenoplax heathiana*) 75- to 83-cell stage (after Heath, 1899, pl. 32, Fig. 23); (F) gastropoda (*Patella vulgata* after Damen and Dictus, 1994 p. 368, Fig. 2D) 64-cell stage; (G) gastropoda (*Calliostoma ligatum*) 56- to 64-cell stage; (H) gastropoda (*Lymnaea stagnalis*, after Verdonk and van den Biggelaar, 1983, p. 111, Fig. 9b). The classical molluscan cross figure formed by cells $1a^{121}-1d^{121}$, $1a^{122}-1d^{122}$ and $2a^{11}-2a^{11}$; (I) aplacophora (*Epimenia verrucosa*, after Baba, 1951 p. 46 Fig. 18, as published in Scheltema, 1993, p. 59, Fig. 1D). (J–L) Annelida: (J) *Amphitrite ornata*, 68-cell stage (after Mead, 1897, pl. XII, Fig. 29). The classical annelid cross is a result of accelerated division (compared to other Eutrochozoa) of the peripheral rosette cells $1a^{112}-1d^{112}$; (K) *Podarke obscura*, 60-cell stage (after Treadwell, 1901, XXXVII, Fig. 17); (L) *Chaetopterus pergamentaceus*, 65-cell stage (after Mead, 1897, pl. XIX Fig. 131).

and $1a^{122}-1d^{122}$ become arranged radially (Fig. 13, yellow). The typical molluscan cross is present only in several gastropod mollusks, for example, *Lymnaea stagnalis* (Fig. 13H) and *Physa fontinalis* (Wierzejski, 1905). However, in many mollusks there is no obvious cross, for example, in the polyplacophoran mollusks *Stenoplax heathiana* (Figs. 13D, E) and *Katharina tunicata* (SAM personal observation), the gastropods *Patella vulgata* (Fig. 13F), *Haliotis tuberculata* (van den Biggelaar, 1993, Fig. 22) and *Calliostoma ligatum* (Fig. 13G) and the neomenioid aplacophoran *Epimenia verrucosa* (Fig. 13I). Various cross-like arrangements might be formed by different cells at different stages, which naturally results from the spiral pattern of cleavage. For instance, in *Stenoplax*, cells of the molluscan cross are formed approximately at the transition from 55- to 63-cell stage (Fig. 13D). Note that large animal cells of the molluscan cross $1a^{121}-1d^{121}$ do not line up in a radial pattern with the vegetal cells $1a^{122}-1d^{122}$. However, at the transition to the 83-cell stage, the animal cells of the cross $1a^{121}-1d^{121}$ divide, so that their daughters line up to form a cross-like pattern (Fig. 13E). Thus, even within the mollusks, there is no definitive developmental stage in which the molluscan cross can be defined, and the classical molluscan cross is apparent in only a few species.

One of the features cited for uniting the sipunculids with mollusks is the presence of a molluscan cross. However, the only sipunculid species for which the early cleavage had been followed in detail is *Golfingia vulgaris* (Fig. 13C). Gerould (1906) in reference to the cleaving embryo of *G. vulgaris* used terminology previously accepted for annelids and called the peripheral rosette cells (blue)—"cross cells" and the cells of the molluscan cross (yellow)—"intermediate cells". Rice (1975, 1985) and Scheltema (1993), however, pointed out that the pattern is more similar to the typical molluscan cross. The presence or absence of the cross is determined by the relative sizes of the different quartet micromeres, for example, if the peripheral rosette cells (blue) are significantly larger than the cells of the molluscan cross (yellow) then the daughters of the latter are forced to form a rather radial structure, which is the case in *Golfingia* (Fig. 13C). The peripheral rosette cells (blue) are small in the mollusks examined (Figs. 10B, C, F, G, J, K) and the cells of the molluscan cross (yellow) lie side by side almost perpendicular to the radii. However, they are radially arranged and form a distinct cross in *L. stagnalis* (Fig. 10G). In this instance, the radial arrangement of the cells of the molluscan cross is due to the large size of the cells of more vegetal quartets. Therefore, the molluscan cross in sipunculids is formed differently and is not comparable to molluscan cross of mollusks.

The annelid cross is as variable in annelids as the molluscan cross is in mollusks (Figs. 13J–L). The classical annelid cross, formed by the large peripheral rosette cells and their progeny (blue) appears in only some annelids, such as *Amphitrite ornata* (Fig. 13J), *Podarke obscura* (Fig. 13K) or *Nereis* spp. (Wilson, 1892). In others, such as *Chaetopterus pergamentaceus* (Fig. 13L), this pattern is not very distinct. In this case, peripheral rosette cells divide obliquely and no classical annelid cross is formed.

Nemerteans resemble sipunculids and annelids in having relatively large peripheral rosette cells (Figs. 13A–B, blue). As in the mollusks *Epimenia*, *Stenoplax*, *Patella* and *Calliostoma*, the cells of the molluscan cross (yellow) do not form a distinct cross-like pattern in nemerteans. On the other hand, a rather distinct cross is formed at the 64-cell stage by the vegetal daughters of the rosette cells $1a^{1112}$–$1d^{1112}$ (Fig. 13A, red) and the animal cells of the molluscan cross (Fig. 13A, yellow). The cross-like pattern becomes even more obvious at the 84-cell stage, when it is formed by the vegetal daughters of the rosette cells $1a^{1112}$–$1d^{1112}$ (Fig. 13B, red) and the animal progeny of the molluscan cross $1a^{1211}$–$1d^{1211}$ (Fig. 13B, yellow), with the peripheral rosette cells (blue) lying between the arms of this "nemertean cross". The feature that seems to be unique to nemertean cleavage is the large size and the accelerated division of the rosette cells $1a^{111}$–$1d^{111}$ (Figs. 13A–B, red) relative to the more vegetal cells of the same generation. The apical rosette cells undergo their seventh division at the 60-cell stage (when the third-quartet micromeres have not yet divided). At the 64-cell stage, their progeny $1a^{1112}$–$1d^{1112}$ and $1a^{1111}$–$1d^{1111}$ are the eight cells located at the apex of the animal hemisphere (Fig. 13A, red).

The presence of the molluscan vs. annelid cross is sometimes treated as two alternative states of a single character in contemporary phylogenetic analyses (Peterson and Eernisse, 2001; Rouse, 1999). However, it is important to understand that cells forming the annelid and molluscan crosses are not homologous (different cell lineages, see Fig. 13) and that cells forming both the molluscan and annelid crosses are present in all spiralian embryos. Coding molluscan and annelid cross as two independent presence/absence characters is problematic because these are just two out of much greater variety of patterns created by the difference in the relative cell size and timing of cell division (see also Jenner, in press). Besides, coding molluscan cross as present in all mollusks (or a hypothetical molluscan ancestor) in an overgeneralization. Although it is difficult to identify the presence or absence of the molluscan vs. annelid cross, several patterns can be recognized from the data in Fig. 13. (1) Mollusks tend to have small peripheral rosette cells (blue) compared to annelids, sipunculids and nemerteans, (2) nemerteans tend to have large apical rosette cells (red), whose division is accelerated relative to the same lineage in annelids, mollusks and sipunculids, (3) annelids have relatively large peripheral rosette cells (blue), whose division is accelerated relative to the same lineage in mollusks, sipunculids and nemerteans. This and other information on the relative timing of division and volume relationships of the quartets (in equal cleavers) or individual cells (in eutrochozoans with unequal cleavage) can be recorded in a form of the character matrix, which can be used for phylogenetic analysis along with other developmental, morphological and molecular characters. Attempts to use information on timing of cell divisions for the inference of phylogeny have already been done on a limited scale (van den Biggelaar and Haszprunar, 1996; Guralnick and Lindberg, 2001). We believe that adding information on the volume relationships can contribute to an even finer resolution for the identification of historical cleavage patterns in eutrochozoan diversification.

Cross-furrow and establishment of bilateral symmetry

The cross-furrow separates opposite blastomeres at the vegetal and animal poles of many spiralian embryos. The presence of the cross-furrow at the four-cell stage is a result of the oblique orientation of spindles of the second cleavage, which produces two "animal" cross-furrow cells (A and C) and two "vegetal" cells (B and D). The absence of the cross-furrow means that the second cleavage is truly meridional (spindles are perpendicular to the animal-vegetal axis of the egg) and all four resulting blastomeres lie in the same plane. In equal-cleaving mollusk embryos, the cross-furrow separating the macromeres plays a key role in biasing the ultimate cell fates of these cells, one of which will ultimately be selected as dorsal (D) macromere (van

den Biggelaar and Guerrier, 1983). While all four of the vegetal macromeres possess the developmental potential to become the D quadrant, typically, it is one of the two vegetal cross-furrow cells because they occupy a more central position in the embryo. This position is favorable for establishing cell contacts with first quartet micromeres that determine the D macromere. Freeman and Lundelius (1992) showed that experimentally increasing the size of one of the macromeres in the equal-cleaving embryo (therefore, increasing the surface of contact with animal micromeres) biases the fate of this macromere towards the formation of D quadrant.

A cross-furrow is often lacking in nemerteans (Henry and Martindale, 1997; Norenburg and Stricker, 2002); however, a review of the older literature and our own observations reveal that there is substantial variation among nemertean species. While the hoplonemerteans *M. grossa* (Hammarsten, 1918), *Zygonemertes virescens* (SAM personal observation), *T. worki* (SAM personal observation), *N. bivittata* (Henry and Martindale, 1995) and the heteronemerteans *Micrura alaskensis* (SAM personal observation) and *C. lacteus* (Henry and Martindale, 1994) do not form a cross-furrow, the hoplonemertean species *E. gracile* (Delsman, 1915) and *A. ochraceus* (SAM personal observation) possess a distinct cross-furrow. In the latter case, we observed formation of a temporary X-furrow as well as substantial variation of the cross-furrow length between the embryos of the same egg batch. Embryos of a hoplonemertean *Oerstedia dorsalis* also form a temporary cross-furrow, although much smaller than in *A. ochraceus* (SAM personal observation). The discovery of a distinct cross-furrow in the palaeonemertean *C. tremaphoros* (Figs. 1A, 5A) may argue for the primitiveness of presence of cross-furrow in the nemertean cleavage. However, a larger sampling of nemertean taxa is necessary to test this assertion.

In contrast to the previously studied nemertean species, *C. lacteus* (Heteronemertea) and *N. bivittata* (Hoplonemertea) (Henry and Martindale, 1994, 1998), the plane of first cleavage in *C. tremaphoros* bears a constant relationship to the plane of bilateral symmetry of the larva. Similar to other spiralians, such as annelids and mollusks, the two cells resulting from the first cleavage consistently produce roughly left-ventral (AB) and right-dorsal (CD) domains of the larval body (Table 2, Figs. 8A–D) (Henry and Martindale, 1999). Although there is a constant relationship of the first two cleavage planes to the larval/adult body axis in *C. tremaphoros*, it is not known whether the fates of these cells are determined at this stage by the segregation of cytoplasmic determinants or whether fates are set up by cell–cell interactions. Recent experimental work on *C. lacteus* (Henry, 2002) argues that the dorso-ventral axis is causally determined by the number of cell interactions between animal and vegetal cells at later cleavage stages. *C. lacteus* does not possess a cross-furrow and thus it is impossible to predict which cells will acquire these inductive interactions. Earlier experiments by Henry and Martindale (1994, 1999) showed that the first cleavage plane in this species can assume two different orientations with respect to the future axis of bilateral symmetry. The presence of a cross-furrow in the palaeonemertean *C. tremaphoros* suggests that features of the spiralian cleavage program that ensure the stereotyped placement of cells into discrete locations within the embryo is an ancient component of eutrochozoan development.

Clonal contributions of the 1st and 2nd quartet micromeres

Four discrete cell quadrants, whose identities are homologous to typical spiralian A, B, C and D quadrants, can be identified in *C. tremaphoros* (Fig. 14). Unlike in other studied spiralians (Boyer et al., 1998; Dictus and Damen, 1997; Render, 1997), but similar to the previously studied heteronemertean *C. lacteus* (Henry and Martindale, 1998), the 1st quartet micromeres are larger (or the same size) as macromeres and generate majority of the larval ectoderm. As in *C. lacteus*, all four quadrants contribute to apical organ. In other spiralians (including *C. lacteus*), progeny of the 1st quartet micromeres are situated along the plane of bilateral symmetry, where the progeny of 1a and 1d lies to the left of medial plane, while 1b and 1c lie to the right. While this arrangement is largely conserved on the ventral side of *C. tremaphoros*, it is modified dorsally, so that the 1d occupies a roughly mid-dorsal position. Another unique feature of *Carinoma*'s development is the oblique position of the trochal lineages with respect to the anterior–posterior axis of the larva. In most other spiralians, the prototroch remains perpendicular to the anterior–posterior axis of the larva even following the gastrulation movements.

As in other spiralians (including *C. lacteus*), progeny of the 2nd quartet micromeres of *C. tremaphoros* are in the ventral (2b), left (2a), dorsal (2d) and right (2c) domains. While micromeres 2a, 2b and 2c each contribute to the three trochoblasts and, possibly, a region of the oesophagus, micromere 2d (the so-called primary somatoblast) produces all of the post-trochal ectoderm, three trochoblasts, and, possibly, the floor of the oesophagus (Fig. 14). While it is said that micromere 2d lies in the dorsal sector, it is meant with respect to the blastopore. Proliferation of the D quadrant result in shifting of the blastopore to the ventral side, so that progeny of the 2d lies dorsally, posteriorly and ventrally in the post-trochal region of the larva. The alternating axial relationships exhibited by successive micromere quartets are characteristic of spiralian development.

Prototroch

One of the most interesting features of development of *C. tremaphoros* is the presence of the prototroch, previously unknown in nemertean larvae (Maslakova and Norenburg, 2001; Maslakova et al., in review). The prototroch is the primary locomotory organ of trochophore larvae and is derived from the same cell lineages across all eutrocho-

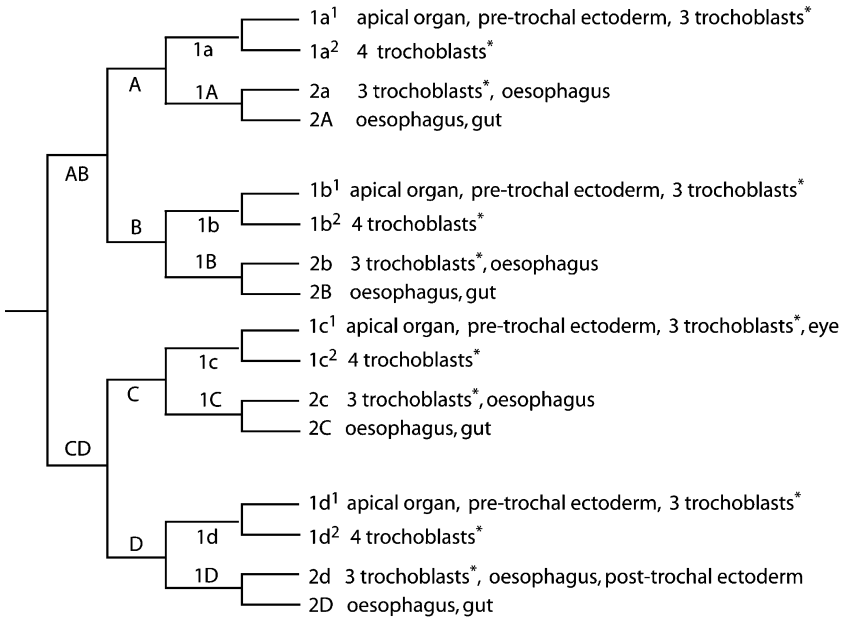

Fig. 14. *Carinoma tremaphoros* lineage diagram summarizing lineage relationships and the larval fates of each cell through the 16-cell stage as determined by the distribution of microinjected fluorescent lineage tracer in 24-h-old larvae. Cell fates are similar to other Eutrochozoa, including origin of the modified prototroch from $1q^1$, $1q^2$ and 2q lineages. Mesodermal origins were not determined. * indicates ultimate degenerative fate of the lineage.

zoan taxa. With the aid of intracellular fluorescent dye injections, we demonstrate here that the large cleavage arrested cells, which are thought to be homologous to the prototroch cells in other spiralians (Maslakova and Norenburg, 2001; Maslakova et al., in review), are derived from the subset of the same lineages ($1q^1$, $1q^2$ and 2q) as in other spiralians (e.g., mollusks and annelids), therefore supporting the assertion of homology. Unlike in the other spiralians, in which the contribution of different quadrants to the formation of the prototroch is unequal (reviewed in Damen and Dictus, 1994), we show here that in *Carinoma*, each of the four quadrants contributes equal number of cells (10) to the prototroch, three of which are derived from the $1q^1$ lineage, four from the $1q^2$ lineage and three from the 2q lineage.

Acknowledgments

We are grateful to Dr. Mary Rice and the staff of the Smithsonian Marine Station at Fort Pierce for their support and assistance. SAM especially would like to acknowledge Eric Edsinger-Gonzales for the fruitful discussions and guidance in the confocal microscopy techniques and Andreas Heyland for his support and assistance on various stages of preparation of the manuscript. This work was partially supported by NSF PEET grant 97124463 to Diana Lipscomb and Jon Norenburg, Link Foundation/Smithsonian Institution Graduate Fellowship to SAM and NSF and NASA grants to MQM. This is contribution No. 576 from the Smithsonian Marine Station at Fort Pierce.

References

Baba, K., 1951. General sketch of the development in a solenogaster, *Epimenia verrucosa* (Nierstrasz). Misc. Repts. Res. Inst. Nat. Res. 19–21, 38–46.

Boyer, B.C., Henry, J.Q., 1998. Evolutionary modifications of the spiralian developmental program. Am. Zool. 38, 621–633.

Boyer, B.C., Henry, J.Q., Martindale, M.Q., 1998. The cell lineage of a polyclad turbellarian embryo reveals close similarity to coelomate spiralians. Dev. Biol. 204, 111–123.

Carson, F., 1990. Histotechnology—A Self-Instructional Text ASCP Press, Chicago, IL.

Casteel, D.B., 1904. The cell-lineage and early development of *Fiona marina*, a nudibranch mollusk. Proc. Acad. Nat. Sci. Philadelphia 56, 325–401.

Child, C.M., 1900. The early development of *Arenicola* and *Sternaspis*. Arch. Entw. -mech. 9, 587–723.

Collier, J.R., 1997. Gastropods, the snails. In: Gilbert, S.F., Raunio, A.M. (Eds.), Embryology, Constructing the Organism. Sinauer Associates, Sunderland, MA, pp. 189–217.

Conklin, E.G., 1897. The embryology of *Crepidula*, a contribution to the cell lineage and early development of some marine gastropods. J. Morphol. 13, 1–266.

Damen, P., Dictus, W.J.A.G., 1994. Cell lineage of the prototroch of *Patella vulgata* (Gastropoda, Mollusca). Dev. Biol. 162, 364–383.

Dawydoff, C., 1928. Sur l'embryologie des *Protonémertes*. C. R. Hebd. Séances. Acad. Sci., Paris 186, 531–533.

Delsman, H.C., 1915. Eifurchung und Gastrulation bei *Emplectonema gracile* Stimpson. Helder. Tijdschr. Ned. Dierkd. Ver. 14, 68–114.

Dictus, W.J.A.G., Damen, P., 1997. Cell lineage and clonal contribution map of the trochophore larva of *Patella vulgata* (Mollusca). Mech. Dev. 62, 213–226.

Freeman, G., Lundelius, J.W., 1992. Evolutionary implications of the mode of D-quadrant specification in coelomates with spiral cleavage. J. Evol. Biol. 5, 205–247.

Friedrich, H.H., 1979. Nemertini. In: Seidel, F. (Ed.), Morphogenese der Tiere. Gustav Fischer Verlag, Stuttgart, pp. 1–136.

Gerould, J.H., 1906. The development of *Phascolosoma* (Studies on the embryology of the Sipunculidae II). Zool. Jahrb., Abt. Anat. Ontog. Tiere 23, 77–162.

Gould-Somero, M., 1975. Echiura. In: Giese, A.C., Pearse, J.S. (Eds.), Reproduction of Marine Invertebrates, vol. 3. Academic Press, New York, pp. 277–311.

Guralnick, R.P, Lindberg, D.R., 2001. Reconnecting cell and animal lineages: what do cell lineages tell us about the evolution and development of Spiralia? Evolution 55, 1501–1519.

Hammarsten, O.D., 1918. Beitrag zur Embryonalentwicklung der *Malacobdella grossa* (Müll.). Inaugural dissertation. Almqvist and Wiksells Boktryckery A.B., Uppsala, p. 96.

Heath, H., 1899. The development of *Ischnochiton*. Zool. Jahrb., Abt. Anat. Ontog. Tiere. 12, 567–656.

Henry, J.J., 2002. Conserved mechanism of dorsoventral axis determination in equal-cleaving spiralians. Dev. Biol. 248, 343–355.

Henry, J.J., Martindale, M.Q., 1994. Establishment of the dorsoventral axis in nemertean embryos—Evolutionary considerations of spiralian development. Dev. Genet. 15, 64–78.

Henry, J.Q., Martindale, M.Q., 1995. The experimental alteration of cell lineages in the nemertean *Cerebratulus lacteus*—Implications for the precocious establishment of embryonic axial properties. Biol. Bull. 189, 192–193.

Henry, J.Q., Martindale, M.Q., 1997. Nemerteans, the ribbon worms. In: Gilbert, S.F., Raunio, A.M. (Eds.), Embryology: Constructing the Organism. Sinauer Associates, Sunderland, MA, pp. 151–166.

Henry, J.J., Martindale, M.Q., 1998. Conservation of the spiralian developmental program: cell lineage of the nemertean, *Cerebratulus lacteus*. Dev. Biol. 201, 253–269.

Henry, J.J., Martindale, M.Q., 1999. Conservation and innovation in spiralian development. Hydrobiologia 402, 255–265.

Iwata, F., 1957. On the early development of the nemertean *Lineus torquatus* Coe. J. Fac. Sci., Hokkaido Univ., Ser. 6, Zoology 13, 54–58.

Iwata, F., 1958. On the development of the nemertean *Micrura akkeshiensis*. Embryologia 4, 103–131.

Iwata, F., 1960. Studies on the comparative embryology of the nemerteans with special reference to their inter-relationships. Publ. Akkeshi Mar. Biol. Stn. 10, 1–51.

Jenner, R.A., in press. Morphological cladistics of the Metazoa: assessing current progress. J. Integr. Comp. Biol.

Jenner, R.A., Schram, F.R., 1999. The grand game of metazoan phylogeny: rules and strategies. Biol. Rev. 74, 121–142.

Lebedinsky, Y.N., 1898. Nabljudenija nad istoriej razvitija nemertin. Zapiski Novorossijkogo Obshchestva Estestvoispytatelej 22, 1–124.

Maslakova, S.A., Malakhov, V.V., 1999. Hidden larva in the Hoplonemertini order of nemerteans. Dokl. Akad. Nauk. 366, 849–852.

Maslakova, S.A., Norenburg, J.L., 2001. Trochophore larva is plesiomorphic for nemerteans: evidence for prototroch in a basal nemertean *Carinoma tremaphoros* (Phylum Nemertea, Palaeonemertea). Am. Zool. 40, 1515–1516.

Maslakova, S.A., Martindale, M.Q. and Norenburg, J.L., In review. The vestigial prototroch in a basal nemertean *Carinoma tremaphoros* (Palaeonemertea, Nemertea).

McBride, E.W., 1914. Text-Book of Embryology MacMilan and Co., Ltd., London.

Mead, A.D., 1897. The early development of marine annelids. J. Morphol. 13, 227–326.

Meisenheimer, J., 1900. Entwicklungsgeschichte von *Dreissena polymorpha*, Pall. Z. Wiss. Zool. 69, 1–137.

Nielsen, C., 2001. Animal Evolution: Interrelationships of the Living Phyla Oxford Univ. Press, Oxford.

Norenburg, J.L., Stricker, S.A., 2002. Phylum Nemertea. In: Young, C.M. (Ed.), Atlas of Marine Invertebrate Larvae. Academic Press, San Diego, CA, pp. 163–177.

Peterson, K.J., Eernisse, D.J., 2001. Animal phylogeny and the ancestry of bilaterians: inferences from morphology and 18s rDNA gene sequences. Evol. Dev. 3, 170–205.

Pilger, J.F., 1997. Sipunculans and Echiurans. In: Gilbert, S.F., Raunio, A.M. (Eds.), Embryology: Constructing the Organism. Sinauer Associates, Sunderland, MA, pp. 167–188.

Reinhardt, H., 1941. Beiträge zur Entwicklungsgeschichte der einheimischen Süßwassernemertine *Prostoma graecense* (Böhmig). Vierteljahrsschr. Nat.forsch. Ges. Zür. 86, 184–252.

Render, J., 1997. Cell fate maps in the *Ilyanassa obsoleta* embryo beyond the third division. Dev. Biol. 189, 301–310.

Rice, M.E., 1975. Sipuncula. In: Giese, A.C., Pearse, J.S. (Eds.), Reproduction of Marine Invertebrates, vol. 2. Academic Press, New York, pp. 67–127.

Rice, M.E., 1985. Sipuncula: developmental evidence for phylogenetic inference. In: Conway Morris, S., Gibson, George R., Platt, H.M. (Eds.), The Origins and Relations of Lower Invertebrates. Oxford Univ. Press, Oxford, UK, pp. 274–296.

Rouse, G.W., 1999. Trochophore concepts: ciliary bands and the evolution of larvae in spiralian Metazoa. Biol. J. Linn. Soc. 66, 411–464.

Scheltema, A.H., 1993. Aplacophora as progenetic aculiferans and the coelomate origin of mollusks as the sister taxon of Sipuncula. Biol. Bull. 184, 57–78.

Schmidt, G.A., 1962. Izmenenie ekologicheskikh otnoshenii u vzrosluikh osobei i evolyutsiya embriogeneza (na primere litoralnuikh nemertin *Lineus desori* (mihi sp.n.) i *Lineus ruber* (O.F. Müller, 1774; G.A. Schmidt, 1945)). Zool. Z. 41, 168–192.

Schmidt, G.A., 1964. Embryonic development of littoral nemertines *Lineus desori* (mihi, sp. nov.) and *Lineus ruber* (O.F. Mülleri, 1774, G.A. Schmidt, 1945) in connection with ecological relation changes of mature individual. Zool. Pol. 14, 75–122.

Schroeder, P.C., Hermans, C.O., 1975. Annelida: Polychaeta. In: Giese, A.C., Pearse, J. (Eds.), Reproduction of Marine Invertebrates, vol. 3. Academic Press, New York, NY, pp. 1–213.

Thollesson, M., Norenburg, J.L., 2003. Ribbon worm relationships—A phylogeny of the phylum Nemertea. Proc. R. Soc. Lond., B Biol. 270, 407–415.

Treadwell, A.L., 1901. The cytogeny of *Podarke obscura*. J. Morphol. 17, 399–486.

van den Biggelaar, J.A.M., 1993. Cleavage pattern in embryos of *Haliotis tuberculata* (Archaeogastropoda) and gastropod phylogeny. J. Morphol. 216, 121–139.

van den Biggelaar, J.A.M., Guerrier, P., 1983. Origin of spatial information. In: Verdonk, N.H., van den Biggelaar, J.A.M., Tompa, A.S. (Eds.), The Mollusca. Academic Press, New York, pp. 179–213.

van den Biggelaar, J.A.M., Haszprunar, G., 1996. Cleavage patterns and mesentoblast formation in the Gastropoda: an evolutionary perspective. Evolution 50, 1520–1540.

Verdonk, N.H., van den Biggelaar, J.A.M., 1983. Early development and the formation of the germ layers. In: Verdonk, N.H., van den Biggelaar, J.A.M., Tompa, A.S. (Eds.), The Mollusca. Academic Press, New York, pp. 91–122.

Wierzejski, A., 1905. Embryologie von *Physa fontinalis*. Z. Wiss. Zool. 83, 502–706.

Wilson, E.B., 1892. The cell lineage of *Nereis:* a contribution to the cytogeny of the annelid body. J. Morphol. 6, 361–480.

Wilson, E.B., 1903. Experiments on cleavage and localization in the nemertean egg. Arch. Entwicklungsmech. 16, 411–458.

Zeleny, C., 1904. Experiments on the localization of developmental factors in the nemertine egg. J. Exp. Zool. 1, 293–329.